LETTER

doi:10.1038/nature23910

# Maternal gut bacteria promote neurodevelopmental abnormalities in mouse offspring

Sangdoo Kim[1]*, Hyunju Kim[1]*, Yeong Shin Yim[2], Soyoung Ha[1], Koji Atarashi[3], Tze Guan Tan[4], Randy S. Longman[5], Kenya Honda[3], Dan R. Littman[6,7], Gloria B. Choi[2] & Jun R. Huh[1]†

**Maternal immune activation (MIA) contributes to behavioural abnormalities associated with neurodevelopmental disorders in both primate and rodent offspring[1–4]. In humans, epidemiological studies suggest that exposure of fetuses to maternal inflammation increases the likelihood of developing autism spectrum disorder[5–7]. In pregnant mice, interleukin-17a (IL-17a) produced by T helper 17 ($T_H17$) cells ($CD4^+$ T helper effector cells involved in multiple inflammatory conditions) induces behavioural and cortical abnormalities in the offspring exposed to MIA[8]. However, it is unclear whether other maternal factors are required to promote MIA-associated phenotypes. Moreover, the underlying mechanisms by which MIA leads to T cell activation with increased IL-17a in the maternal circulation are not well understood. Here we show that MIA phenotypes in offspring require maternal intestinal bacteria that promote $T_H17$ cell differentiation. Pregnant mice that had been colonized with mouse commensal segmented filamentous bacteria or human commensal bacteria that induce intestinal $T_H17$ cells were more likely to produce offspring with MIA-associated abnormalities. We also show that small intestine dendritic cells from pregnant, but not from non-pregnant, females secrete IL-1β, IL-23 and IL-6 and stimulate T cells to produce IL-17a upon exposure to MIA. Overall, our data suggest that defined gut commensal bacteria with a propensity to induce $T_H17$ cells may increase the risk of neurodevelopmental disorders in the offspring of pregnant mothers undergoing immune system activation owing to infections or autoinflammatory syndromes.**

In mouse models of MIA, offspring born to pregnant dams that were exposed to viral infection or injected with a synthetic double-stranded RNA (polyinosinic:polycytidylic acid, poly(I:C)) that mimics viral infection exhibit abnormal behavioural phenotypes, including reduced sociability, increased repetitive behaviours, and abnormal communication[3,4]. As commensal microbiota influences immune responses to pathogenic microbes, we sought to determine whether it affects the likelihood of a mother producing offspring with MIA-associated phenotypes.

As previously reported[8–10], pups from mothers injected with poly(I:C) at embryonic day 12.5 (E12.5) emit more ultrasonic vocalization (USV) calls than those from PBS-injected mothers (Fig. 1a). Unlike other behavioural phenotypes that are often more strongly manifested in male than in female offspring, USV calls were enhanced in both sexes among MIA offspring (Extended Data Fig. 1a). In addition, fetal exposure to MIA led to other behavioural abnormalities, including enhanced repetitive behaviours (increased marble burying), increased anxiety (decreased time spent in the centre of an open field arena) and social interaction deficits (decreased interaction with a social stimulus) in adult male offspring (Fig. 1b–d). These behavioural phenotypes did not emerge from changes in activity or arousal levels as the total investigation time and the total distance travelled during the sociability test remained comparable (Extended Data Fig. 1b, c). To investigate whether maternal commensal bacteria influence MIA-associated behaviours, we treated wild-type C57BL/6 mice from our vivarium with the broad spectrum antibiotic vancomycin before phosphate-buffered saline (PBS) or poly(I:C) administration (Extended Data Fig. 1d). Pre-treatment of poly(I:C)-injected mothers with vancomycin prevented development of all four behavioural abnormalities in MIA offspring (Fig. 1a–d).

We previously showed that MIA offspring exhibit cortical patches devoid of cortical-layer-specific markers, such as SATB2 (ref. 8), and these cortical patches resemble lesions described in brains of patients with autism spectrum disorder[11,12]. These cortical patches are predominantly localized in the area encompassing the dysgranular zone of the primary somatosensory cortex and are closely associated with MIA-associated behavioural abnormalities[30]. Unlike the adult offspring derived from poly(I:C)-injected dams, the offspring of poly(I:C)-injected mothers pre-treated with vancomycin failed to develop cortical patches (Fig. 1e, Extended Data Fig. 1e, f). Vancomycin treatment of poly(I:C)-injected pregnant dams led to a decrease in the proportion of $T_H17$ cells in the small intestine with a concomitant reduction in the levels of IL-17a in the maternal plasma compared to those of the control group (Fig. 1f, Extended Data Fig. 1g). These data indicate that the presence in pregnant mice of commensal bacteria that are sensitive to vancomycin is crucial for the induction of MIA-associated behavioural and brain abnormalities in the offspring. Furthermore, the presence of such bacteria is associated with increased proportion of $T_H17$ cells in the small intestine and high levels of IL-17a in the plasma of poly(I:C)-treated pregnant dams.

Among commensal bacteria in laboratory mice, segmented filamentous bacteria (SFB) are susceptible to vancomycin[13] and contribute disproportionately to $T_H17$ cell biogenesis in the small intestine[14]. Indeed, qPCR analyses of mouse faecal samples showed that intestinal colonization by SFB is severely reduced upon vancomycin treatment (Extended Data Fig. 1h). We also performed scanning electron microscopy to visualize SFB associated with intestinal epithelial cells[14]. Although SFB were found attached to the ileal mucosa of the PBS-treated dams, SFB associated with intestinal epithelial cells were not detected in the vancomycin-treated dams (Extended Data Fig. 1i). We therefore next investigated whether the presence of SFB in pregnant mice correlated with the MIA-associated behavioural phenotypes in

[1]Division of Infectious Diseases and Immunology and Program in Innate Immunity, Department of Medicine, University of Massachusetts Medical School, Worcester, Massachusetts 01605, USA. [2]The McGovern Institute for Brain Research, Department of Brain and Cognitive Sciences, Massachusetts Institute of Technology, Cambridge, Massachusetts 02139, USA. [3]Department of Microbiology and Immunology, Keio University School of Medicine, Tokyo 160-8582, Japan. [4]Department of Microbiology and Immunobiology, Harvard Medical School, Boston, Massachusetts 02115, USA. [5]The Jill Roberts Institute for Research in IBD, Division of Gastroenterology and Hepatology, Weill Cornell Medicine, New York, New York 10021, USA. [6]The Kimmel Center for Biology and Medicine of the Skirball Institute, New York University School of Medicine, New York, New York 10016, USA. [7]Howard Hughes Medical Institute, New York, New York 10016, USA.
†Present address: Division of Immunology, Department of Microbiology and Immunobiology and Evergrande Center for Immunological Diseases, Harvard Medical School and Brigham and Women's Hospital, Boston, Massachusetts 02115, USA.
*These authors contributed equally to this work.

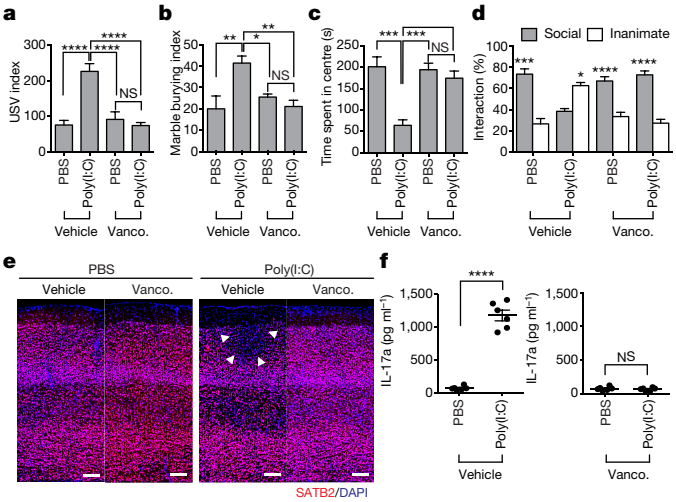


**Figure 1 | Maternal bacteria promote abnormal behaviours associated with neurodevelopmental disorders in MIA offspring. a**, USV index ($n = 28$, 34 (vehicle; PBS, poly(I:C)); $n = 26$, 30 (vancomycin (Vanco.); PBS, poly(I:C)); 5–6 independent experiments). **b**–**d**, Marble burying index (**b**), time spent in the centre of an open field (**c**), percentage of interaction in the sociability test (**d**) of adult offspring described in **a** ($n = 13$, 15 (vehicle; PBS, poly(I:C)); $n = 12$, 16 (vancomycin; PBS, poly(I:C)); 3–4 independent experiments). **e**, Representative images of adult offspring brains from PBS-, poly(I:C)-injected mothers treated with vehicle or vancomycin. Arrowheads indicate cortical patch. Scale bar, 100 μm ($n = 3$, 4 (PBS; vehicle, vancomycin); $n = 5$, 4 (poly(I:C); vehicle, vancomycin); 2 independent experiments). **f**, Maternal plasma concentrations of IL-17a 48 h after PBS, poly(I:C) administration into dams at E12.5 ($n = 6$ per group; 3 independent experiments). $^{*}P < 0.05$, $^{**}P < 0.01$, $^{***}P < 0.001$, $^{****}P < 0.0001$ calculated by one-way (**a**–**c**) and two-way (**d**) ANOVA with Tukey post hoc tests and Student's *t*-test (**f**). NS, not significant. Graphs indicate mean ± s.e.m.

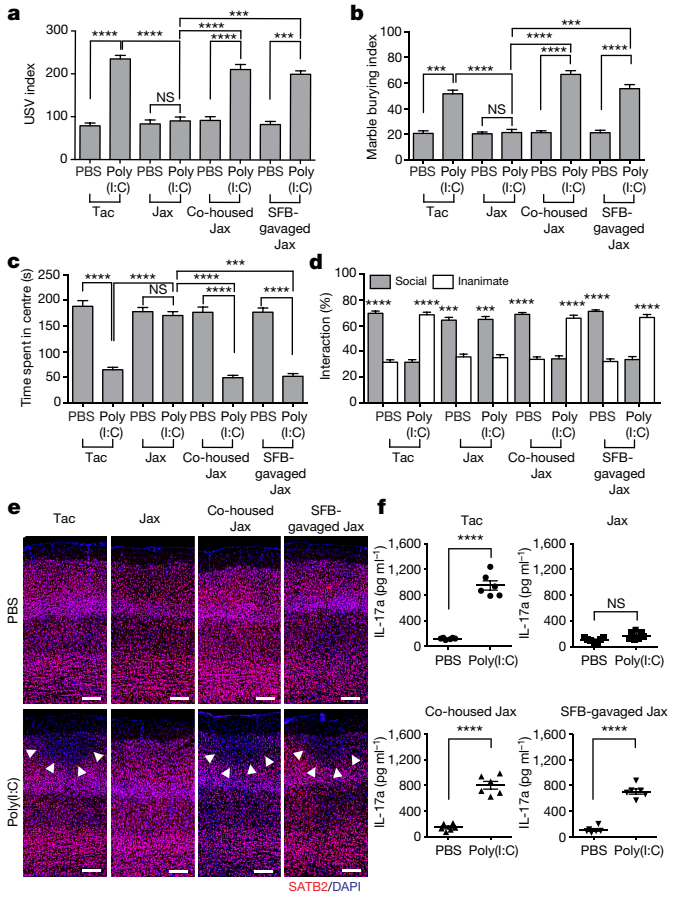


**Figure 2 | SFB in the pregnant mothers promotes abnormal behaviours in MIA offspring. a**, USV index ($n = 59$, 125 (Tac; PBS, poly(I:C)); $n = 51$, 50 (Jax; PBS, poly(I:C)); $n = 55$, 81 (co-housed Jax; PBS, poly(I:C)); $n = 55$, 89 (SFB-gavaged Jax; PBS, poly(I:C)); 9–11 independent experiments). **b**–**d**, Marble burying index (**b**), time spent in the centre of an open field (**c**), and percentage of interaction in the sociability test (**d**) of adult offspring described in **a** ($n = 32$, 50 (Tac; PBS, poly(I:C)); $n = 29$, 27 (Jax; PBS, poly(I:C)); $n = 29$, 29 (co-housed Jax; PBS, poly(I:C)); $n = 33$, 30 (SFB-gavaged Jax; PBS, poly(I:C)); 7–8 independent experiments). **e**, Representative images of adult offspring brains from PBS-, poly(I:C)-injected mothers ($n = 3$, 3 (PBS; Tac, Jax); $n = 3$, 3 (PBS; co-housed Jax, SFB-gavaged Jax); $n = 4$, 3 (poly(I:C); Tac, Jax); $n = 3$, 3 (poly(I:C); co-housed Jax, SFB-gavaged Jax)). Arrowheads indicate cortical patches. Scale bar, 100 μm. **f**, Maternal plasma concentrations of IL-17a 48 h after administration of PBS, poly(I:C) into dams at E12.5 ($n = 6$ per group; 2 independent experiments). $^{***}P < 0.001$, $^{****}P < 0.0001$ calculated by one-way (**a**–**c**) and two-way (**d**) ANOVA with Tukey post hoc tests and Student's *t*-test (**f**). NS, not significant. Graphs indicate mean ± s.e.m.

offspring. C57BL/6 mice from Taconic Biosciences (Tac) have abundant $T_H17$ cells in their small intestine owing to the presence of SFB; in contrast, C57BL/6 mice from Jackson Laboratories (Jax), which lack SFB, have few intestinal $T_H17$ cells[13,14]. Unlike offspring from poly(I:C)-injected Tac mothers, those from poly(I:C)-injected Jax mothers did not show any of the MIA-associated behavioural phenotypes (Fig. 2a–d, Extended Data Fig. 2a, b). Poly(I:C)-treated Tac and Jax mothers had litters of similar sizes and the pups had similar weights (Extended Data Fig. 2c, d). Sizes of the cortical patches observed in the offspring of poly(I:C)-injected Tac mothers were highly correlated with the severity of the MIA-associated behavioural abnormalities[30]. Consistent with this finding, MIA offspring from the SFB-deficient Jax mothers injected with poly(I:C) had no cortical abnormalities, as assessed by SATB2 staining (Fig. 2e, Extended Data Fig. 2e, f). Unlike in Tac mice, Jax mothers injected with poly(I:C) did not show systemic increases in IL-17a in the plasma (Fig. 2f). However, poly(I:C) injection of both Tac and Jax animals resulted in the robust induction of TNFα and IFNβ, compared to PBS-injected control mice (Extended Data Fig. 2g).

Offspring of poly(I:C)-injected Jax mothers that had been either co-housed with Tac mice or gavaged with a faecal slurry from SFB mono-colonized mice (Extended Data Fig. 3a) displayed MIA-associated behavioural and cortical abnormalities (Fig. 2a–e). These MIA-associated phenotypes in the offspring from both the co-housed and SFB-gavaged Jax mothers were accompanied by an increased proportion of gut-residing $T_H17$ cells, consistent with the presence of SFB in the small intestines of these mice (Extended Data Fig. 3b–d). Accordingly, the co-housed and SFB-gavaged Jax mothers exhibited increased levels of plasma IL-17a following poly(I:C) injections (Fig. 2f). Thus, the presence or absence of a single commensal bacterial species SFB in the intestines of pregnant mothers influences long-lasting behavioural and neurodevelopmental outcomes in the offspring exposed to MIA.

We next investigated whether maternal exposure to poly(I:C)-induced inflammation or maternal colonization with SFB influence MIA-associated behaviours in offspring after birth. We performed cross-fostering experiments by switching newborns between PBS- and poly(I:C)-treated Tac mothers or between SFB-positive Tac and SFB-negative Jax mothers (Extended Data Figs 4a, 5a). Whereas offspring derived from poly(I:C)-injected mothers, but reared by PBS-injected mothers, exhibited behavioural abnormalities, those from PBS-injected mothers that were reared by poly(I:C) mothers exhibited normal behaviours (Extended Data Fig. 4b–g). Likewise, offspring derived from poly(I:C)-injected Tac mothers, but reared by Jax mice, exhibited behavioural abnormalities, whereas those derived from poly(I:C)-injected Jax mothers and reared by Tac mothers displayed normal behaviours (Extended Data Fig. 5b–g). These data indicate

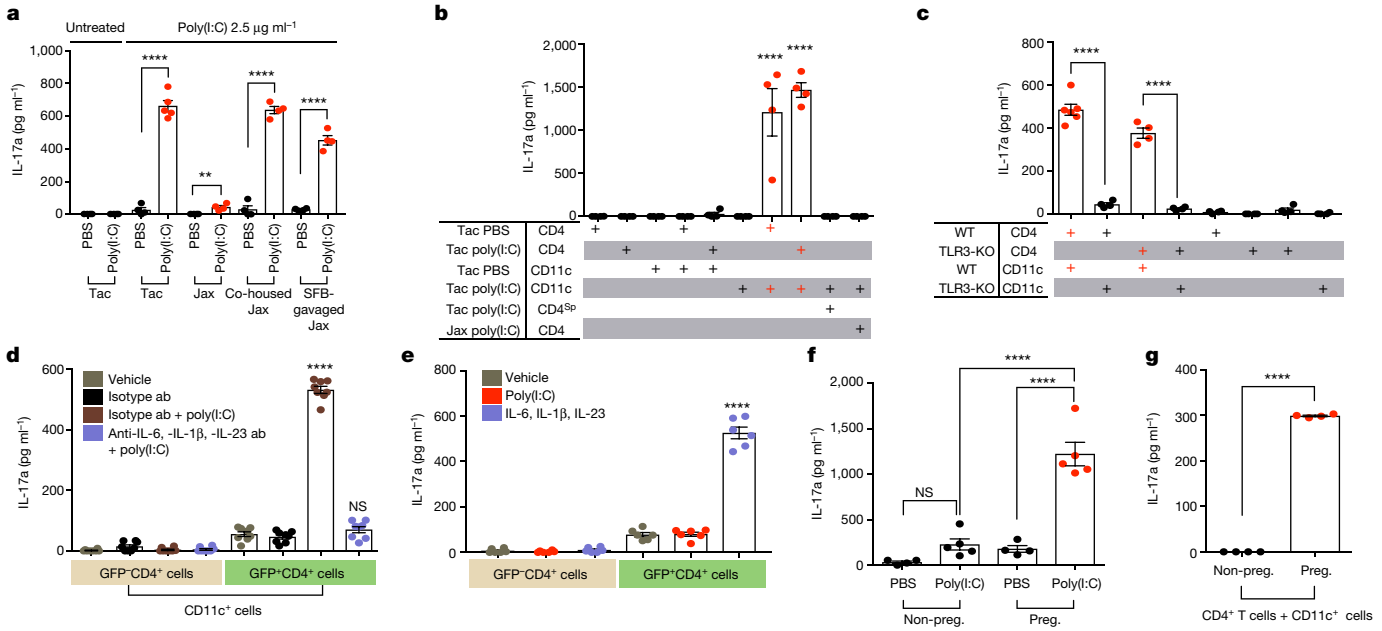


**Figure 3 | SFB-specific T cells are the major IL-17a producer in pregnant mothers treated with poly(I:C).** **a**–**e**, **g**, Supernatant concentrations of IL-17a from *ex vivo* cultured mononuclear cells of ilea in PBS- or poly(I:C)-treated dams (**a**) ($n = 4$–5 per group), from co-culture of $CD4^+$ and $CD11c^+$ of ilea in PBS- or poly(I:C)-treated Tac or Jax mice (**b**) ($n = 4$ per group), from co-cultures of $CD4^+$ and $CD11c^+$ of ilea in poly(I:C)-treated wild-type or TLR3-KO mice (**c**) ($n = 4$–6 per group), from co-cultures of $GFP^+CD4^+$, $GFP^-CD4^+$ and $CD11c^+$ from ilea of poly(I:C)-treated *Il17a*$^{GFP}$ mice (**d**) ($n = 8$ per group), from sorted $GFP^+CD4^+$ and $GFP^-CD4^+$ cells (**e**) ($n = 6$ per group), or from co-cultures of $CD4^+$ and $CD11c^+$ (**g**) ($n = 4$ per group). $CD4^{Sp}$, spleen-derived $CD4^+$ T cells. All cultured cells were isolated at E14.5 and stimulated with poly(I:C) for 18 h (**a**–**c**, **g**) or for 48 h (**d**, **e**). **f**, Maternal plasma concentrations of IL-17a 48 h after administration of PBS or poly(I:C) into non-pregnant females or dams at E12.5 ($n = 4$, 5 (non-pregnant females; PBS, poly(I:C)); $n = 4$, 5 (pregnant females; PBS, poly(I:C))). All data pooled from 2 independent experiments. $^{**}P < 0.01$, $^{****}P < 0.0001$ calculated by one-way (**a**–**f**) ANOVA with Tukey post hoc tests and Student's *t*-test (**g**). NS, not significant. Graphs indicate mean ± s.e.m.

that both the presence of SFB in the small intestines of mothers and the immunological effects of poly(I:C) are critical during pregnancy, not during post-natal nursing, for licensing MIA-induced behavioural abnormalities in offspring.

MIA leads to an increase in plasma IL-17a levels in pregnant mice as early as 12–24 h following E12.5 poly(I:C) injection[8]. Such a rapid increase strongly suggested that pre-existing $T_H17$ cells, rather than *de novo* differentiating $T_H17$ cells, are the major source for IL-17a in pregnant mice exposed to inflammation. As $T_H17$ cells are most abundant in the small intestine lamina propria, we next investigated whether poly(I:C) stimulates IL-17a production via gut-residing $T_H17$ cells. In poly(I:C)-treated pregnant mice, T cells isolated from lamina propria, but not spleens or mesenteric lymph nodes, expressed high levels of IL-17a and had increased RORγt expression compared to cells from PBS-treated mice (Extended Data Fig. 6a–f). Consistent with these observations, ileum-associated mononuclear cells, isolated from poly(I:C)-injected Tac pregnant mice and further stimulated *in vitro* with poly(I:C), produced higher levels of IL-17a compared to those from PBS-treated Tac mice (Fig. 3, Extended Data Fig. 6g). In contrast, mononuclear cells from poly(I:C)-treated Jax mice secreted only small amounts of IL-17a (Fig. 3a). Introduction of SFB into Jax mice either by co-housing them with Tac mice or by gavage with an SFB-containing faecal slurry was sufficient to enable ileum-associated mononuclear cells to produce high levels of IL-17a (Fig. 3a). To examine which cells are involved in the poly(I:C) response, we separately isolated $CD4^+$ and non-$CD4^+$ cells from PBS- and poly(I:C)-treated pregnant Tac mice and co-cultured the isolated cells from each experimental group. The $CD4^-$ fraction derived from the poly(I:C)-treated, but not from the PBS-treated, mothers promoted IL-17a production when added to cultures containing $CD4^+$ cells from either PBS- or poly(I:C)-treated pregnant mice (Extended Data Fig. 6h). We next tested whether poly(I:C)-primed $CD11c^+$ dendritic cells (DCs) were capable of stimulating $CD4^+$ T cells to produce IL-17a. Adding $CD11c^+$ DCs derived from poly(I:C)-treated, but not from PBS-treated, pregnant mice to *ex vivo* cultures containing ileal $CD4^+$ T cells that were isolated from either PBS- or poly(I:C)-treated pregnant Tac mice led to robust expression of IL-17a (Fig. 3b). In contrast, neither splenic $CD4^+$ T cells of poly(I:C)-injected pregnant Tac mice nor ileal $CD4^+$ T cells of poly(I:C)-injected pregnant Jax mice produced IL-17a, even with the help of $CD11c^+$ DCs (Fig. 3b). Thus, both $CD4^+$ T cells present in the small intestines of Tac mice and poly(I:C)-activated $CD11c^+$ DCs are required for robust IL-17a induction. Among the multiple phenotypes of gut-residing DCs, $CD103^+CD11b^+CD11c^+$ cells were robust inducers of IL-17a when co-cultured with ileal $CD4^+$ T cells (Extended Data Fig. 6i), consistent with previous reports[15,16].

As poly(I:C) activates Toll-like receptor 3 (TLR3)[17], we investigated whether this receptor is involved in stimulation of IL-17a production. Whereas $CD4^+$ T cells, regardless of their *Tlr3* genotype, produced IL-17a when mixed with wild-type $CD11c^+$ DCs, they failed to do so when co-cultured with TLR3-deficient $CD11c^+$ DCs (Fig. 3c). In addition, poly(I:C) injection of TLR3-KO pregnant mice failed to induce MIA-associated USV phenotypes in offspring (Extended Data Fig. 6j). These data suggest that MIA-associated phenotypes require functional TLR3 expression on $CD11c^+$ DCs.

Inflammatory cytokines such as IL-1β, IL-6, and IL-23 enhance the function and differentiation of $T_H17$ cells[18]. Consistent with this, co-cultures of sorted $CD4^+$ and $CD11c^+$ DCs that were isolated from the ilea of poly(I:C)-treated pregnant Tac mice and incubated with IL-1β-, IL-6-, and IL-23-blocking antibodies failed to produce IL-17a, even when supplemented with poly(I:C) (Fig. 3d). In contrast, $GFP^+$ $T_H17$ cells, but not $GFP^-$ non-$T_H17$ cells, sorted from the ilea of IL-17a–GFP reporter mice produced high levels of IL-17a in the presence of exogenous IL-1β, IL-6, and IL-23, even in the absence of

poly(I:C)-treated CD11c$^+$ DCs (Fig. 3e). Collectively, these data indicate that poly(I:C) treatment leads to the activation of gut-residing CD103$^+$CD11b$^+$CD11c$^+$ cells, which stimulate poised $T_H17$ cells to produce IL-17a through secretion of IL-1β, IL-6, and IL-23.

Intriguingly, we noted that poly(I:C) injection of non-pregnant females failed to increase the levels of plasma IL-17a (Fig. 3f). Co-culture of ileal CD4$^+$ and CD11c$^+$ DCs isolated from poly(I:C)-treated pregnant females, but not from poly(I:C)-treated non-pregnant females, resulted in secretion of IL-17a *ex vivo* (Fig. 3g). Consistent with these findings, gut CD11c$^+$ DCs isolated from poly(I:C)-treated pregnant females, but not from poly(I:C)-treated non-pregnant females, produced increased levels of IL-1β, IL-6, and IL-23 (Extended Data Fig. 6k). Together, these data collectively suggest that $T_H17$-cell-inducing gut bacteria, a pro-inflammatory stimulus, and pregnancy are all required for the systemic increase in IL-17a in maternal plasma, and this increase in IL-17a promotes MIA-associated behavioural and neurodevelopmental abnormalities in offspring.

We next investigated whether commensal-antigen-specific $T_H17$ cells in pregnant mothers were sufficient to induce MIA-associated phenotypes in the offspring. Congenically marked naive CD45.1$^+$CD4$^+$ T cells from mice expressing a transgenic T cell receptor (TCR) specific for a SFB-encoded antigen (7B8-Tg)[19] were adoptively transferred into SFB-colonized CD45.2$^+$ recipient mice lacking αβ T cells (TCRα-KO) or deficient in IL-17a production (IL-17a-KO) (Extended Data Fig. 7a). In line with our previous findings that $T_H17$ cells are critical mediators of MIA[8], offspring derived from poly(I:C)-injected TCRα-KO mothers crossed with wild-type C57BL/6 fathers failed to exhibit MIA-induced behavioural phenotypes. On the other hand, offspring from TCRα KO pregnant mothers that had received naive 7B8-Tg CD4$^+$ T cells exhibited MIA-associated behavioural phenotypes even in the absence of exposure to poly(I:C)-induced inflammation (Extended Data Fig. 7b). We subsequently tested whether IL-17a produced by the SFB antigen-specific CD4$^+$ T cells was sufficient to induce MIA phenotypes in offspring by transferring these cells into IL-17a-KO females[20]. Unlike the offspring from the poly(I:C)-treated IL-17a-KO mothers that had been crossed with wild-type C57BL/6 fathers, offspring of poly(I:C)-injected IL-17a-KO mothers that had received 7B8-Tg CD4$^+$ T cells displayed all four MIA-associated behavioural abnormalities (Extended Data Fig. 7c). In addition, offspring from 7B8-Tg CD4$^+$ T cell recipient females exhibited the cortical phenotype (Extended Data Fig. 7d–h). Induction of the MIA behavioural phenotypes was accompanied by an increase in IL-17a in the maternal plasma (Extended Data Fig. 7i, j) and increased IL-17a production from SFB-specific donor CD45.1$^+$ T cells, but not from CD45.2$^+$ T cells of IL-17a-KO recipient mice (Extended Data Fig. 7k). Therefore, these results indicate that microbiota-specific gut $T_H17$ cells present in pregnant mice are sufficient to produce abnormal behavioural and neurodevelopmental phenotypes in the offspring when accompanied by strong signalling for IL-17a production in the mother.

Finally, we investigated whether gut-residing bacteria isolated from humans could also promote MIA-associated phenotypes in mice. Administration of a mix of twenty different commensal bacteria isolated from human faecal samples was previously shown to induce $T_H17$ cells in the large intestines of mice[21]. We orally gavaged Jax mothers with a mix of these twenty human bacterial strains twice, on E3.5 and E10.5, followed by a poly(I:C) injection at E12.5 (Extended Data Fig. 8a). Introduction of the twenty strains led to stable colonization of 2–10 commensal bacteria (Supplementaty Table 1) and, as previously shown[21], to an increased percentage of $T_H17$ cells in the colons of the recipient mice (Extended Data Fig. 8b). Unlike in the SFB-colonized Jax mice, we could not detect SFB in the ilea of the recipient mice (Extended Data Fig. 8c). Importantly, poly(I:C) injection of the human-bacteria-gavaged Jax mice induced high levels of IL-17a in the maternal plasma and MIA-associated abnormal behavioural and nerurodevelopmental phenotypes in the offspring (Fig. 4, Extended Data Fig. 8d–g). These MIA-associated phenotypes were not observed if the mothers were pre-treated with IL-17a-blocking antibody (Fig. 4, Extended Data Fig. 8d–g).

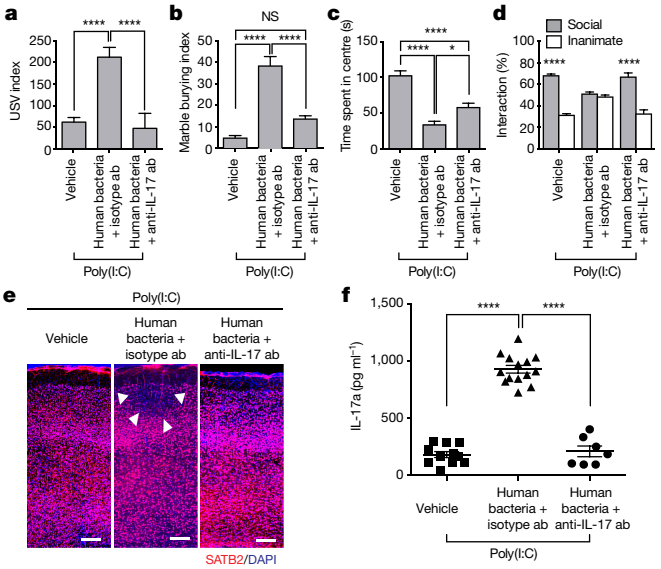


**Figure 4 | Human commensal bacteria inducing gut $T_H17$ cells promote abnormal behavioural phenotypes in MIA offspring.** **a**, USV index ($n = 38$, 32, 27 for vehicle-gavaged only/human-bacteria-gavaged + isotype control antibody/human-bacteria-gavaged + anti-IL-17a antibody; 6 independent experiments). **b**–**d**, Marble burying index (**b**), time spent in the centre of an open-field (**c**), and percentage of interaction (**d**) ($n = 23$, 22, 13 for vehicle-gavaged only/human-bacteria-gavaged + isotype control antibody/human-bacteria-gavaged + anti-IL-17a antibody; 4 independent experiments). **e**, Representative SATB2 staining in the cortex of the offspring derived from vehicle/human-bacteria-gavaged Jax dams. Arrowheads indicate cortical patches. Scale bar, 100 μm. **f**, Maternal plasma concentrations of IL-17a at E14.5 ($n = 7$–14 per group; 2 independent experiments). $^*P < 0.05$, $^{****}P < 0.0001$ calculated by one-way (**a**–**c**, **f**) or two-way (**d**) ANOVA with Tukey post-hoc tests. NS, not significant. Graphs indicate mean ± s.e.m.

There have been several recent reports of individual human commensal bacteria that promote differentiation of intestinal $T_H17$ cells[22,23]. Unlike offspring from Jax mothers colonized with *Listeria monocytogenes* or *Bacteroides fragilis*, in which there is no induction of $T_H17$ cells, offspring of mice colonized with $T_H17$-cell-inducing *Bifidobacterium adolescentis* or an adherent *Escherichia coli* isolate, CD-SpA 2A, emitted enhanced USV calls (Extended Data Fig. 9a–c). The presence of MIA-associated behavioural phenotypes in offspring correlated with increased IL-17a in the plasma of poly(I:C)-injected mothers (Extended Data Fig. 9d). On the other hand, pregnant mice gavaged with *L. monocytogenes* had increased IFNγ production (Extended Data Fig. 9e). None of these human-bacteria-gavaged mothers were colonized with SFB (Extended Data Fig. 9f). Thus, intestinal $T_H17$ cell induction by individual human commensal bacteria contributes to the development of MIA-associated abnormality in mouse offspring.

Accumulating evidence suggests that the gut commensal microbiota have roles in autoimmune diseases and cancer[24–26]. Moreover, intricate relationships exist between the bacterial community in the gastrointestinal tract and the central nervous system[27–29]. Our findings extend our understanding of the potential of microbiota to influence the likelihood of a mother having offspring with neurodevelopmental disorders. Women with gut microbial communities that promote excessive $T_H17$ cell differentiation may therefore be more likely to bear children with autistic spectrum disorder in the event of pathological inflammation during pregnancy. A better understanding of the role of the maternal microbiota and pregnancy-associated changes in gut-residing immune

cells may provide opportunities to reduce the risk of inflammation-induced neurodevelopmental disorders.

**Online Content** Methods, along with any additional Extended Data display items and Source Data, are available in the online version of the paper; references unique to these sections appear only in the online paper.

**Received 12 December 2016; accepted 16 August 2017.**
**Published online 13 September 2017.**

1. Machado, C. J., Whitaker, A. M., Smith, S. E., Patterson, P. H. & Bauman, M. D. Maternal immune activation in nonhuman primates alters social attention in juvenile offspring. *Biol. Psychiatry* **77,** 823–832 (2015).
2. Bauman, M. D. *et al.* Activation of the maternal immune system during pregnancy alters behavioral development of rhesus monkey offspring. *Biol. Psychiatry* **75,** 332–341 (2014).
3. Smith, S. E. P., Li, J., Garbett, K., Mirnics, K. & Patterson, P. H. Maternal immune activation alters fetal brain development through interleukin-6. *J. Neurosci.* **27,** 10695–10702 (2007).
4. Malkova, N. V., Yu, C. Z., Hsiao, E. Y., Moore, M. J. & Patterson, P. H. Maternal immune activation yields offspring displaying mouse versions of the three core symptoms of autism. *Brain Behav. Immun.* **26,** 607–616 (2012).
5. Lee, B. K. *et al.* Maternal hospitalization with infection during pregnancy and risk of autism spectrum disorders. *Brain Behav. Immun.* **44,** 100–105 (2015).
6. Brown, A. S. *et al.* Elevated maternal C-reactive protein and autism in a national birth cohort. *Mol. Psychiatry* **19,** 259–264 (2014).
7. Atladóttir, H. O. *et al.* Maternal infection requiring hospitalization during pregnancy and autism spectrum disorders. *J. Autism Dev. Disord.* **40,** 1423–1430 (2010).
8. Choi, G. B. *et al.* The maternal interleukin-17a pathway in mice promotes autism-like phenotypes in offspring. *Science* **351,** 933–939 (2016).
9. Schwartzer, J. J. *et al.* Maternal immune activation and strain specific interactions in the development of autism-like behaviors in mice. *Transl. Psychiatry* **3,** e240 (2013).
10. Yee, N., Schwarting, R. K., Fuchs, E. & Wöhr, M. Increased affective ultrasonic communication during fear learning in adult male rats exposed to maternal immune activation. *J. Psychiatr. Res.* **46,** 1199–1205 (2012).
11. Casanova, M. F. *et al.* Focal cortical dysplasias in autism spectrum disorders. *Acta Neuropathol. Commun.* **1,** 67 (2013).
12. Stoner, R. *et al.* Patches of disorganization in the neocortex of children with autism. *N. Engl. J. Med.* **370,** 1209–1219 (2014).
13. Ivanov, I. I. *et al.* Specific microbiota direct the differentiation of IL-17-producing T-helper cells in the mucosa of the small intestine. *Cell Host Microbe* **4,** 337–349 (2008).
14. Ivanov, I. I. *et al.* Induction of intestinal $T_H17$ cells by segmented filamentous bacteria. *Cell* **139,** 485–498 (2009).
15. Lewis, K. L. *et al.* Notch2 receptor signaling controls functional differentiation of dendritic cells in the spleen and intestine. *Immunity* **35,** 780–791 (2011).
16. Persson, E. K. *et al.* IRF4 transcription-factor-dependent $CD103^+CD11b^+$ dendritic cells drive mucosal T helper 17 cell differentiation. *Immunity* **38,** 958–969 (2013).
17. Alexopoulou, L., Holt, A. C., Medzhitov, R. & Flavell, R. A. Recognition of double-stranded RNA and activation of NF-κB by Toll-like receptor 3. *Nature* **413,** 732–738 (2001).
18. Awasthi, A. & Kuchroo, V. K. $T_H17$ cells: from precursors to players in inflammation and infection. *Int. Immunol.* **21,** 489–498 (2009).
19. Yang, Y. *et al.* Focused specificity of intestinal $T_H17$ cells towards commensal bacterial antigens. *Nature* **510,** 152–156 (2014).
20. Nakae, S. *et al.* Antigen-specific T cell sensitization is impaired in IL-17-deficient mice, causing suppression of allergic cellular and humoral responses. *Immunity* **17,** 375–387 (2002).
21. Atarashi, K. *et al.* $T_H17$ cell induction by adhesion of microbes to intestinal epithelial cells. *Cell* **163,** 367–380 (2015).
22. Tan, T. G. *et al.* Identifying species of symbiont bacteria from the human gut that, alone, can induce intestinal $T_H17$ cells in mice. *Proc. Natl Acad. Sci. USA* **113,** E8141–E8150 (2016).
23. Viladomiu, M. *et al.* IgA-coated *E. coli* enriched in Crohn's disease spondyloarthritis promote $T_H17$-dependent inflammation. *Sci. Transl. Med.* **9,** eaaf9655 (2017).
24. Lee, Y. K., Menezes, J. S., Umesaki, Y. & Mazmanian, S. K. Proinflammatory T-cell responses to gut microbiota promote experimental autoimmune encephalomyelitis. *Proc. Natl Acad. Sci. USA* **108** (Suppl 1), 4615–4622 (2011).
25. Wu, H. J. *et al.* Gut-residing segmented filamentous bacteria drive autoimmune arthritis via T helper 17 cells. *Immunity* **32,** 815–827 (2010).
26. Sivan, A. *et al.* Commensal *Bifidobacterium* promotes antitumor immunity and facilitates anti-PD-L1 efficacy. *Science* **350,** 1084–1089 (2015).
27. Erny, D. *et al.* Host microbiota constantly control maturation and function of microglia in the CNS. *Nat. Neurosci.* **18,** 965–977 (2015).
28. Diaz Heijtz, R. *et al.* Normal gut microbiota modulates brain development and behavior. *Proc. Natl Acad. Sci. USA* **108,** 3047–3052 (2011).
29. Cryan, J. F. & Dinan, T. G. Mind-altering microorganisms: the impact of the gut microbiota on brain and behaviour. *Nat. Rev. Neurosci.* **13,** 701–712 (2012).
30. Yim, Y. S. *et al.* Reversing behavioural abnormalities in mice exposed to maternal inflammation. *Nature* http://dx.doi.org/nature23909 (2017).

**Supplementary Information** is available in the online version of the paper.

**Acknowledgements** We thank S. Hang, D. Paik and N. Silverstein for valuable discussions and Y. Yang, M. Xu, N. Geva-Zatorsky, D. Kasper, C. Benoist and D. Mathis for reagents. We thank M. Trombly, N. Silverstein and A. Park for critical reading of the manuscript. We also thank E. Bridge, E. Jaskolski and other staff members at the Department of Animal Medicine at University of Massachusetts Medical School. This work was supported by the Simons Foundation Autism Research Initiative 274443 (D.R.L.) and 402005 (J.R.H.), the Simons Foundation to the Simons Center for the Social Brain at MIT (Y.S.Y., J.R.H and G.B.C.), Hock E. Tan and K. Lisa Yang Center for Autism Research (G.B.C.), the Howard Hughes Medical Institute (D.R.L.), Robert Buxton (G.B.C.), the National Research Foundation of Korea grants MEST-35B-2011-1-E00012 (S.K.) and NRF-2014R1A1A1006089 (H.K.), the Searle Scholars Program (J.R.H.), the Pew Scholar for Biomedical Sciences (J.R.H.), the Kenneth Rainin Foundation (J.R.H.), and the National Institutes of Health grants R01DK106351 and R01DK110559 (J.R.H.).

**Author Contributions** S.K., T.G.T., R.S.L., K.H., D.R.L., G.B.C. and J.R.H. designed the experiments and/or provided advice, reagents and technical expertise. S.K., H.K., Y.S.Y., S.H. and K.A. performed the experiments. S.K., G.B.C. and J.R.H. wrote the manuscript with inputs from the co-authors.

**Author Information** Reprints and permissions information is available at www.nature.com/reprints. The authors declare no competing financial interests. Readers are welcome to comment on the online version of the paper. Publisher's note: Springer Nature remains neutral with regard to jurisdictional claims in published maps and institutional affiliations. Correspondence and requests for materials should be addressed to G.B.C. (gbchoi@mit.edu) and J.R.H. (jun_huh@hms.harvard.edu).

**Reviewer Information** *Nature* thanks C. Powell, M. Prinz and the other anonymous reviewer(s) for their contribution to the peer review of this work.

## METHODS

**Data reporting.** Sample sizes were determined on the basis of similarly conducted studies. For experiments administering mice with PBS and poly(I:C) or vehicle and bacteria, mice were randomly assigned into two groups matched for sex and age. The investigators were blinded to allocation during experiments and outcome assessment for all the behavioural assays except for the experiments with human bacteria.

**Animals.** All experiments were performed according to Guide for the Care and Use of Laboratory Animals and were approved by the National Institutes of Health and the Committee and Animal Care at University of Massachusetts Medical School. C57BL/6, *Tcra*$^{KO}$, *Tlr3*$^{KO}$, *Il17a*$^{GFP}$ and SFB-specific TCR transgenic (7B8-Tg) mice were purchased from Taconic biosciences and Jackson Laboratory. To induce MIA phenotypes, SFB were introduced into mice purchased from Jackson laboratory. *Il17a*$^{KO}$ mice were described elsewhere[20].

**Maternal immune activation.** Mice were mated overnight and females were checked daily for the presence of seminal plugs, noted as embryonic day 0.5. On E12.5, pregnant female mice were weighed and injected with a single dose (20 mg kg$^{-1}$; i.p.) of poly(I:C) (Sigma Aldrich) or PBS vehicle. Each dam was returned to its cage and left undisturbed until the birth of its litter. All pups remained with the mother until weaning on postnatal day 21–28 (P21–P28), at which time mice were group housed at a maximum of 5 per cage with same-sex littermates.

**Co-housing, SFB-gavaged and antibiotics-gavaged mice.** For co-housing experiments, age-matched SFB-absent mice (from Jackson Laboratory) were co-housed with SFB-present mice (from Taconic Biosciences) in sterilized cages for two weeks at a ratio of 2:3, with unrestricted access to food and water. For SFB-gavaging experiments, four faecal pellets of SFB mono-colonized mice (provided by D.R.L.) were dissolved in 20 ml sterile PBS and filtered though a 100-μm cell strainer. 200 μl of faecal suspensions were gavaged via oral route to 4-week-old female Jackson mice. Control mice were gavaged with PBS. The SFB colonization was tested on day 7 following co-housing or SFB-gavaging. For ablation of intestinal bacteria, Taconic-derived female mice were orally gavaged with vancomycin hydrochloride (Fisher) (2.5 mg kg$^{-1}$) every two days, starting 7 days before breeding. Mouse faecal pellets were collected and stored at −80 °C before and after vancomycin treatments.

**Mice gavaged with human commensal bacteria.** Twenty human-associated $T_H17$-inducing bacterial strains were isolated from faecal samples of a patient with ulcerative colitis[21]. Fifteen strains (1A9, 1F8, 1D2, 1F7, 1D4, 2D9, 2E3, 2E1, 1D10, 1E3, 2H6, 2G4, 2G11, 1B11 and 1C2) were grown on Reinforced Clostridial Agar (Oxoid), two strains (1C12, 1E11) were on GAM Agar (Nissui), two strains (1D1, 2F7) were on Schaedler Agar (BD), and one strain (2H11) was on Tryptic Soy Agar (BD). Two days after plating, microbes were scraped from agar plates, suspended in 5 ml of 20% glycerol in PBS, and mixed with equal number of live bacteria (approximately final concentrations of $5 \times 10^8$ CFU ml$^{-1}$ of each strain). The mixture of twenty bacterial strains were stored at −80 °C until use. Pregnant Jax mice were inoculated twice by oral gavage at E3.5 and E10.5, with 200–300 μl of bacterial suspension. For the IL-17 cytokine blockade experiment, monoclonal IL-17a-blocking antibody (clone 50104; R&D) or isotype control antibody (IgG2a, clone 54447; R&D) were administered 8 h before maternal immune activation via i.p. route (300 μg per animal). For colonization with *B. fragilis*, *B. adolescentis* and adherent *E. coli* CD-SpA 2A, pregnant Jax mice were inoculated three times by oral gavages at E4.5, E6.5 and E8.5 with 200 μl of bacteria suspension. (approximately final concentrations of $1 \times 10^9$ CFU ml$^{-1}$ of each strain). Bacterial stocks were prepared as previously described[22,23].

***Listeria*-gavaged mice.** *Listeria monocytogenes*[19] was cultured in BHI broth media (Sigma, cat. no 35286 CFU). Pregnant Jax mice were inoculated three times by oral gavages at E4.5, E6.5 and E8.5 with 200 μl of bacteria suspension (approximately final concentrations of $2 \times 10^9$ CFU ml$^{-1}$). Colonization levels were determined by collecting mouse faecal samples at E12.5, re-suspending them with PBS and subsequently plating on BHI agar.

**Cross-fostering.** The day on which pups were born was considered P0. Pups were cross-fostered between P0 and P1. Whole litters were removed from the original mothers. Pups were gently mixed with the bedding of the new cage. Pups were then introduced to the new cage with a foster mother. Pups from PBS- and poly(I:C)-treated Taconic mothers were cross-fostered to poly(I:C)- and PBS-treated Taconic mothers, respectively. Additionally, pups from Taconic- and Jax-derived mothers were cross-fostered to a Jax- and Taconic-derived dam, respectively.

**Behavioural assays.** All behavioural testing were carried out according to the previously established behavioural schemes[8] with minor modifications. Blinding was performed for all the behavioural experiments except for the experiments with human bacteria.

**Ultrasonic vocalizations.** On P9, both male and female offspring mice were removed from the nest and habituated to the testing room for 30 min. After the habituation period, mouse pups were placed in a clean 15-cm glass Pyrex high wall dish. Ultrasonic vocalizations (USVs) were detected for 3 min using an UltraSoundGateCM16/CMPA microphone (AviSoft) in the sound attenuation chamber under stable temperature and light control, and recorded with SAS Prolab software (AviSoft). USVs were measured between 33–125 kHz using Ultravox software (Noldus Information Technology, USA). Owing to the unreliability of automated USV scoring, all pup USV calls were counted manually and plotted on the *y* axis. As both male and female pups of poly(I:C)-injected mothers emitted comparable levels of USVs (Extended Data Fig. 1a), we did not separately analyse male versus female USV phenotypes. Both sexes were used for the experiments.

**Three-chamber social approach.** 8–12-week-old male mice were tested for social behaviour using the three-chamber social approach paradigm. Experimental mice were habituated for 1 h in separate clean holding cages and then introduced into a three-chamber arena with only empty object-containment cages (circular metallic cages, Stoelting Neuroscience) for a total 10-min acclimation phase in two 5-min sessions. The following day, the mice were placed in the centre chamber (without access to the left and right social test areas) and allowed to explore the centre area for 5 min. After this exploration period, barriers to adjacent chambers were removed, allowing mice to explore the left and right arenas, which contained a social object (unfamiliar C57BL/6 male mouse) in one chamber and an inanimate object (black rubber stopper) in the other chamber. Experimental mice were given 10 min to explore both chambers and measured for approach behaviour as interaction time (that is, sniffing, approach) with targets in each chamber (within 2 cm). Sessions were video-recorded and object exploration time and total distance moved were analysed using the Noldus tracking system. Percentage interaction was calculated as the percentage of time spent investigating the social stimulus out of the total exploration time of both objects (Supplementary Table 2) and plotted on the *y* axis. Arenas and contents were thoroughly cleaned between testing sessions. Multiple social targets from different home cages were used for testing to prevent potential odorant confounds from target home cages.

**Marble burying test.** Male mice were placed in a testing arena (arena size: $40 \times 20$ cm$^2$, bedding depth: 3 cm) containing 20 glass marbles, which were laid out in four rows of five marbles equidistant from one another. At the end of a 15 min exploration period, mice were gently removed from the testing cages and the number of marbles buried was recorded. A marble burying index was scored as 1 for marbles covered >50% by bedding, 0.5 for around 50% covered, or 0 for anything less. Percentage of buried marbles is plotted on the *y* axis.

**Open field test.** Mice underwent a 15-min exploration period in the testing arena (arena size: $50 \times 50$ cm$^2$). Sessions were video-recorded and analysed for time spent in the centre (centre size: $25 \times 25$ cm$^2$) using EthoVision Noldus tracking system (Noldus). Time spent in the centre of an open field is plotted on the *y* axis.

**Immunohistochemistry.** Adult male mice were perfused and fixed with 4% paraformaldehyde in PBS overnight at 4 °C. The brains were removed and sectioned at 50 μm thickness with a Leica VT100S vibratome (Leica). Slices were permeabilized with blocking solution containing 0.4% Triton X-100, 2% goat serum, and 1% BSA in PBS for 1 h at room temperature, and then incubated with anti-SATB2 (special AT-rich sequence-binding protein 2) (ab51502, Abcam) antibodies overnight at 4 °C. The following day, slices were incubated with fluorescently conjugated secondary antibodies (Invitrogen) for 1 h at room temperature, and mounted in Vectashield mounting medium with DAPI (Vector Laboratories). Images of stained brain slices were acquired using a confocal microscope (LSM710. Carl Zeiss) with a 20× objective lens. The cortical malformation images were analysed using ImageJ software. The images were cropped to have S1 cortical patches in the centre.

**Analysis of cortical patches.** Cortical patches were identified as cortical regions devoid of SATB2 expression. The size of the cortical patches in the S1 was calculated using Zen software (Carl Zeiss). The cortical region was divided into 10 equal laminar blocks representing different depths of the cortex. SATB2 positive cells were quantified manually.

**Scanning electron microscopy.** Terminal ileum tissues from mice (12–14 weeks old) were cut open and fixed with 2.5% glutaraldehyde in 0.1 M cacodylate buffer (pH 7.4) overnight and processed for standard scanning electron microscopy at the EM centre, University of Massachusetts Medical School. All samples were analysed on a Hitachi S-4800 Type II Field Emission Scanning Electron Microscope.

**16S rRNA quantitative PCR analysis.** Bacterial genomic DNA was isolated from the faecal pellets of mice with phenol-chloroform extraction. qPCR was performed to quantify relative abundance of SFB, human commensal bacteria or total bacteria using group specific 16S rDNA primers (Supplementaty Table 3). Undetected qPCR values from non-colonized samples were replaced with a $C_t$ value of 40 for the purpose of comparison.

**Lamina propria mononuclear cell preparation.** For mononuclear cell isolations, both mesenteric fat tissues and Peyer's patches were carefully removed

from intestinal tissues. Terminal ileal or colonic tissues were incubated in 5 mM EDTA in PBS containing 1 mM DTT at 37 °C on a shaker (200 r.p.m.) for 20 min. Tissues were washed one more time. Tissues were then further digested for 30 min at 37 °C in RPMI containing 10% fetal bovine serum, 1.0 mg $ml^{-1}$ collagenase D (Roche) and 100 μg $ml^{-1}$ DNase I (Sigma). Digested tissues were then filtered using a 100 μm cell strainer and incubated for additional 10 min at 37 °C. Mononuclear cells were isolated from an interphase of percoll gradients (40:80 gradient).

**Flow cytometry.** Mononuclear cells were incubated with or without 50 ng $ml^{-1}$ phorbol myristate acetate (PMA) (Sigma) and 500 ng $ml^{-1}$ ionomycin (Sigma) in the presence of GolgiStop (BD) in complete T cell media at 37 °C for 5 h. Intracellular cytokine staining was performed according to the manufacturer's protocol. Cells were stained with Pacific-Blue-conjugated anti-CD4 (RM-5), PerCP-Cy5.5-conjugated anti-CD8a (53-6.7), APC-Cy7-conjugated anti-TCRβ (H57-597), FITC-conjugated anti-CD62L (MEL-14), APC-conjugated anti-CD44 (IM7), PE-conjugated-CD25 (PC61.5), PerCP-Cy5.5-conjugated-CD19 (eBio1D3), APC-conjugated anti-CD45.1 (A20), FITC-conjugated anti-CD45.2 (104), Pacific-Blue-conjugated anti-CD11c (N418), FITC-conjugated-anti-CD11b (M1/70), PerCP-Cy5.5-conjugated-anti-CD103 (2E7) (eBioscience), Biotin-conjugated Vβ14 (14-2) (BD phamigen) and PE-Cy7-conjugated-Streptavidin (Thermo Fisher Scientific). Cells were further stained intracellularly with APC-conjugated anti-RORγ (B2D) (eBioscience) and PE-Cy7-conjugated anti-IL-17a (eBio17B7) (eBioscience) using Foxp3 staining/permeabilization buffer (eBioscience). Flow cytometric analysis was performed on an LSRII (BD Biosciences). All data were re-analysed using FlowJo (Tree Star).

**Adoptive transfer.** Spleen and lymph nodes from 7B8-Tg mice were collected and disassociated. Red blood cells were lysed using ACK lysis buffer (Lonza). Naive $CD4^+$ T cells ($CD62L^{hi}CD44^{lo}TCRv\beta14^+CD4^+CD19^-$) from $CD45.1^+$ 7B8-Tg mice were sorted on a BD FACS Aria II. Sorted $5 \times 10^4$ cells were transferred into congenic CD45.2 recipient mice by tail vein injection.

**Cell sorting.** Mononuclear cells were isolated at E14.5 from small intestines of poly(I:C)-treated pregnant $Il17a^{GFP}$ or C57BL/6 mice. $GFP^+$ and $GFP^-$ T cells, gated on $CD8^-CD19^-TCR\beta^+CD4^+$, were sorted with a FACSAria (BD biosciences). DCs were stained with antibodies and sorted based on their surface expression of CD103 and CD11b (gated on $CD4^-CD8^-CD19^-MHCII^+CD11c^+$).

***Ex vivo* mononuclear cell culture.** Mononuclear cells isolated from ilea of either PBS- or poly(I:C)-treated mice on E14.5 were cultured *in vitro* with poly(I:C) (2.5 μg $ml^{-1}$). $CD4^+$ or $CD11c^+$ cells were positively selected using microbeads (Miltenyi). For co-culture assay, $CD4^+$ cells ($1.5–3.5 \times 10^4$ cells $ml^{-1}$) were cultured with $CD11c^+$ DCs ($7.5–16 \times 10^4$ cells $ml^{-1}$) at 1:5 ratio in each well. $CD4^+$ and $CD11c^+$ cells were incubated for 24–48 h with IgG antibody (20 ng $ml^{-1}$) or with anti-IL-1β antibody (20 ng $ml^{-1}$), anti-IL-6 antibody (20 ng $ml^{-1}$) and anti-IL-23p19 antibody (20 ng $ml^{-1}$) (R&D System) with or without poly(I:C) stimulation (2.5 μg $ml^{-1}$) (Sigma). $CD4^+$ cells were cultured with recombinant IL-1β (10 ng $ml^{-1}$), IL-6 (5 ng $ml^{-1}$) and IL-23 (5 ng $ml^{-1}$) (R&D System). All cells were cultured in T cell media: RPMI 1640 (Invitrogen) supplemented with 10% (v/v) heat-inactivated FBS (Hyclone) and 50 U penicillin–streptomycin (Invitrogen). Cell culture supernatant was used for ELISA analyses.

**ELISA.** IL-17a, TNFα, IFNβ, IL-1β and IL-23 levels were measured according to the manufacturer's protocol (BioLegend). IL-6 and IFNγ levels were measured according to the manufacturer's protocol (eBioscience).

**Statistics.** Statistical analyses were performed using GraphPad Prism. ANOVAs were followed by Tukey or Sidak tests. All data are represented as mean ± s.e.m. Sample sizes were determined on the basis of similarly conducted studies[8]. When conducting behavioural assays, cages were pseudo-randomly assigned for tests. Detailed statistical analyses for behavioural assays are included in the Supplementary Information.

**Data availability.** Source Data are available in the online version of the paper. All other data are available from the corresponding author upon reasonable request.

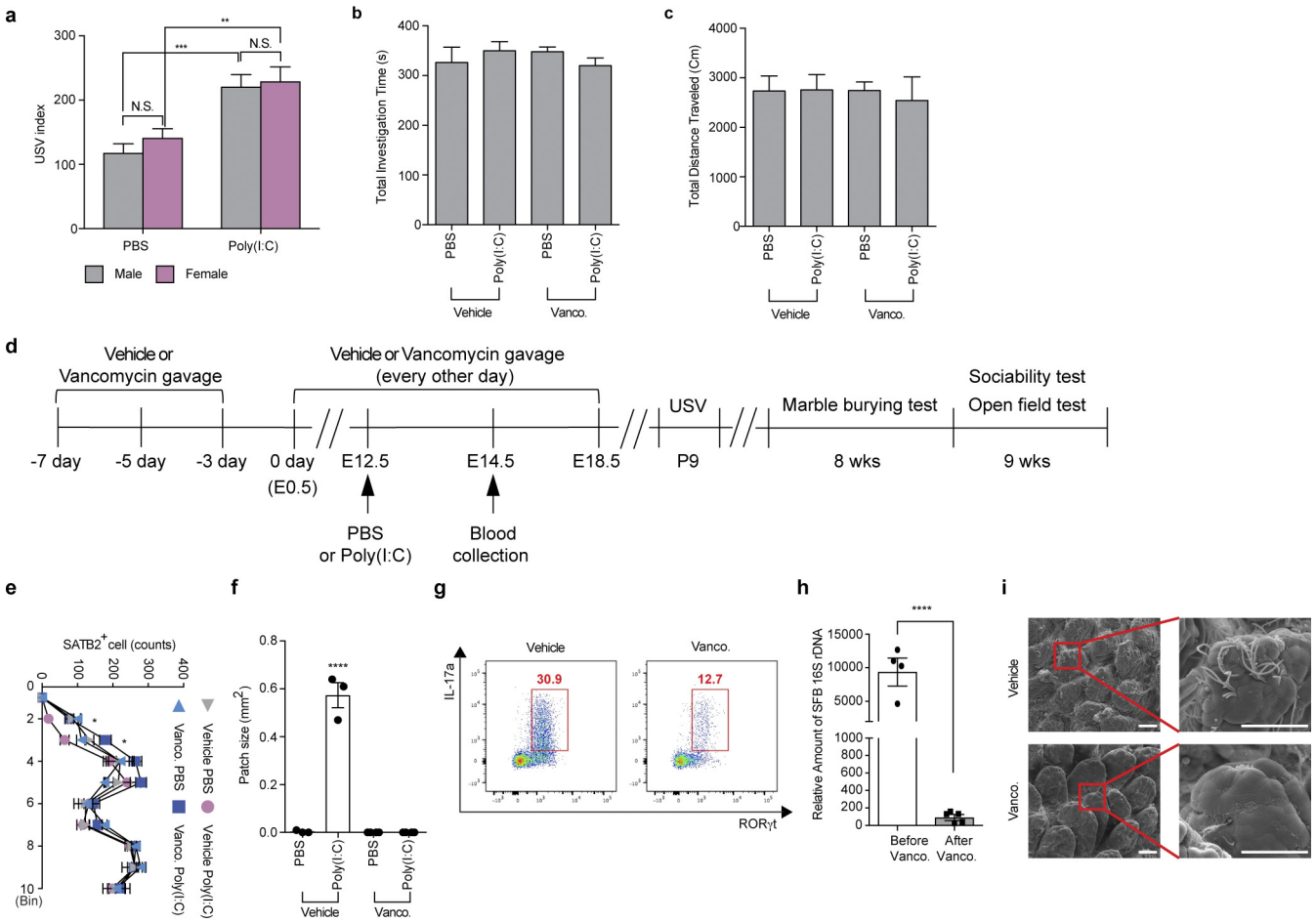


**Extended Data Figure 1 | Maternal vancomycin-treatment prevented induction of behavioural abnormalities in MIA offspring. a**, USV index ($n = 27, 29$ (PBS; male, female); $n = 28, 21$ (poly(I:C); male, female); 6 independent experiments). **b**, **c**, Total investigation time (**b**) and total distance travelled (**c**) during the sociability test ($n = 13, 15$ (vehicle; PBS, poly(I:C)); $n = 12, 16$ (vancomycin; PBS, poly(I:C)); 3–4 independent experiments). **d**, Schematic of the experimental design. **e**, **f**, Quantification of SATB2$^+$ cells (**e**) in the cortex divided into ten equal bins representing different depths of the cortex or of the cortical patch size (**f**) in the primary somatosensory cortex (S1) ($n = 3, 4$ (PBS; vehicle, vancomycin); $n = 3, 4$ (poly(I:C); vehicle, vancomycin); 2 independent experiments). **g**, Flow cytometry of CD4$^+$ T cells (gated on TCRβ$^+$CD4$^+$) stained intracellularly for IL-17a and RORγt. Mononuclear cells were collected at E14.5 from the ilea of poly(I:C)-treated mice with/without vancomycin treatment; representative FACS plot from 3 independent experiments. **h**, qPCR analysis measuring relative SFB levels in C57BL/6 mice before/after vancomycin treatments ($n = 4–5$ per group). **i**, Representative s.e.m. images of epithelial surfaces in the ilea of the vehicle-/vancomycin-treated mice from 2 independent experiments. Scale bars, 30 μm. $^*P < 0.05$, $^{**}P < 0.01$, $^{***}P < 0.001$, $^{****}P < 0.0001$ calculated by two-way (**a**, **e**) and one-way (**b**, **c**, **f**) ANOVA with Tukey post hoc tests. NS, not significant. Graphs indicate mean ± s.e.m.

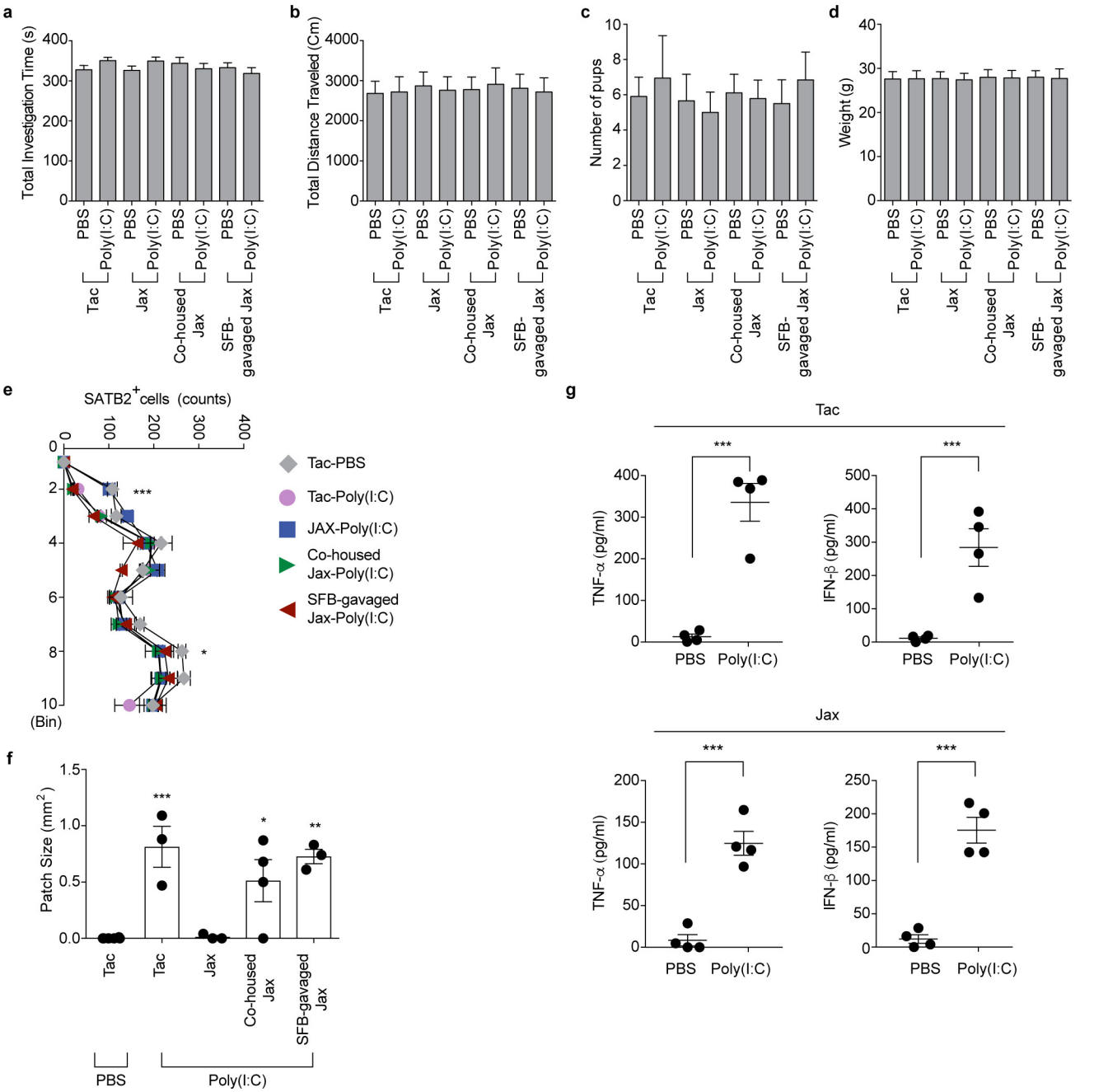


**Extended Data Figure 2 | MIA in SFB-absent Jax mothers does not induce changes in the total activity of the adult offspring, properties of the litter and maternal cytokine production.** **a**, **b**, Total investigation time (**a**) and total distance travelled (**b**) during the sociability test of adult offspring described in Fig. 2b–d. **c**, Litter size upon weaning ($n = 59$, 125 (Tac; PBS, poly(I:C)); $n = 51$, 50 (Jax; PBS, poly(I:C)); $n = 55$, 81 (co-housed Jax; PBS, poly(I:C)); $n = 55$, 89 (SFB-gavaged Jax; PBS, poly(I:C)). **d**, Weight of male offspring from the groups described in **c** ($n = 32$, 50 (Tac; PBS, poly(I:C)); $n = 29$, 27 (Jax; PBS, poly(I:C)); $n = 29$, 29 (co-housed Jax; PBS, poly(I:C)); $n = 33$, 30 (SFB-gavaged Jax; PBS, poly(I:C)). Data in **c** and **d** are from 7–8 independent experiments. **e**, **f**, Quantification of SATB2$^+$ cells (**e**) in the cortex divided into ten equal bins representing different depth and of patch size (**f**) in the S1 ($n = 4$ (Tac; PBS); $n = 3$, 3, 4, 3 (Tac, Jax, co-housed Jax, SFB-gavaged Jax; poly(I:C)). **g**, Maternal plasma concentrations of TNFα and IFNβ at 3 h after PBS, poly(I:C) injection into Tac/Jax dams at E12.5; $n = 4$ per group. $^*P < 0.05$, $^{**}P < 0.01$, $^{***}P < 0.001$ calculated by two-way (**e**) and one-way ANOVA (**a**–**d**, **f**) with Tukey post hoc tests and Student's *t*-test (**g**). Graphs indicate mean ± s.e.m.

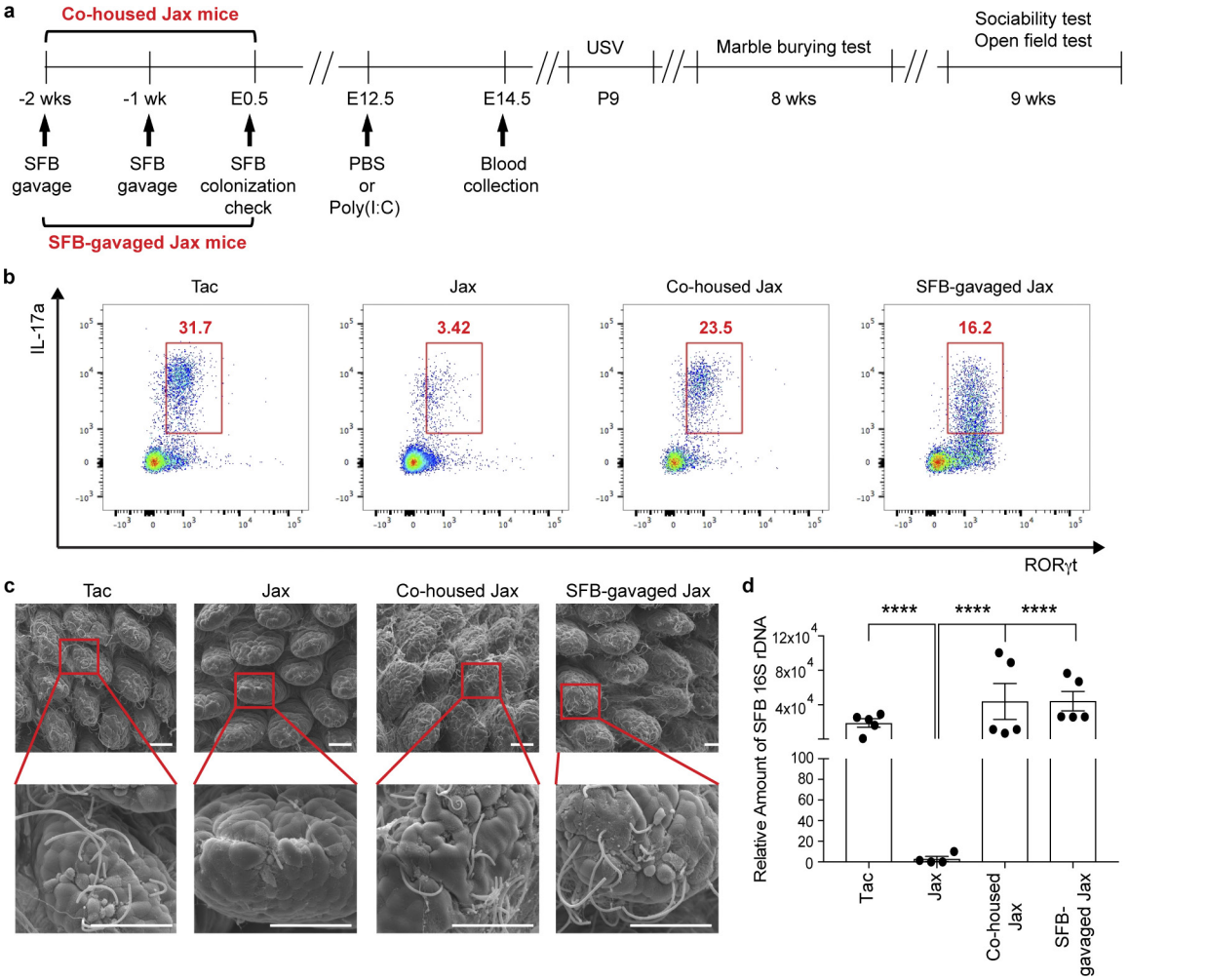


**Extended Data Figure 3 | SFB colonization leads to increased levels of gut $T_H17$ cells in Jax pregnant mice. a**, Schematic of the experimental design. **b**, Flow cytometry of $CD4^+$ T cells (gated on $TCR\beta^+CD4^+$) stained intracellularly for IL-17a and RORγt. Mononuclear cells were collected at E14.5 from the ilea of poly(I:C)-treated Tac, Jax, co-housed Jax, SFB-gavaged Jax mothers. **c**, Representative s.e.m. images of epithelial surfaces in the ilea of Tac, Jax, co-housed Jax, SFB-gavaged Jax mothers. Scale bars, 30 μm. Data representative of 3 (**b**) and 2 (**c**) independent experiments. **d**, qPCR analysis for SFB levels in the faecal samples of the groups described in (**a**) ($n = 4–5$ per group). $^{****}P < 0.0001$ calculated by one-way (**d**) ANOVA with Tukey post hoc test. Graphs indicate mean ± s.e.m.

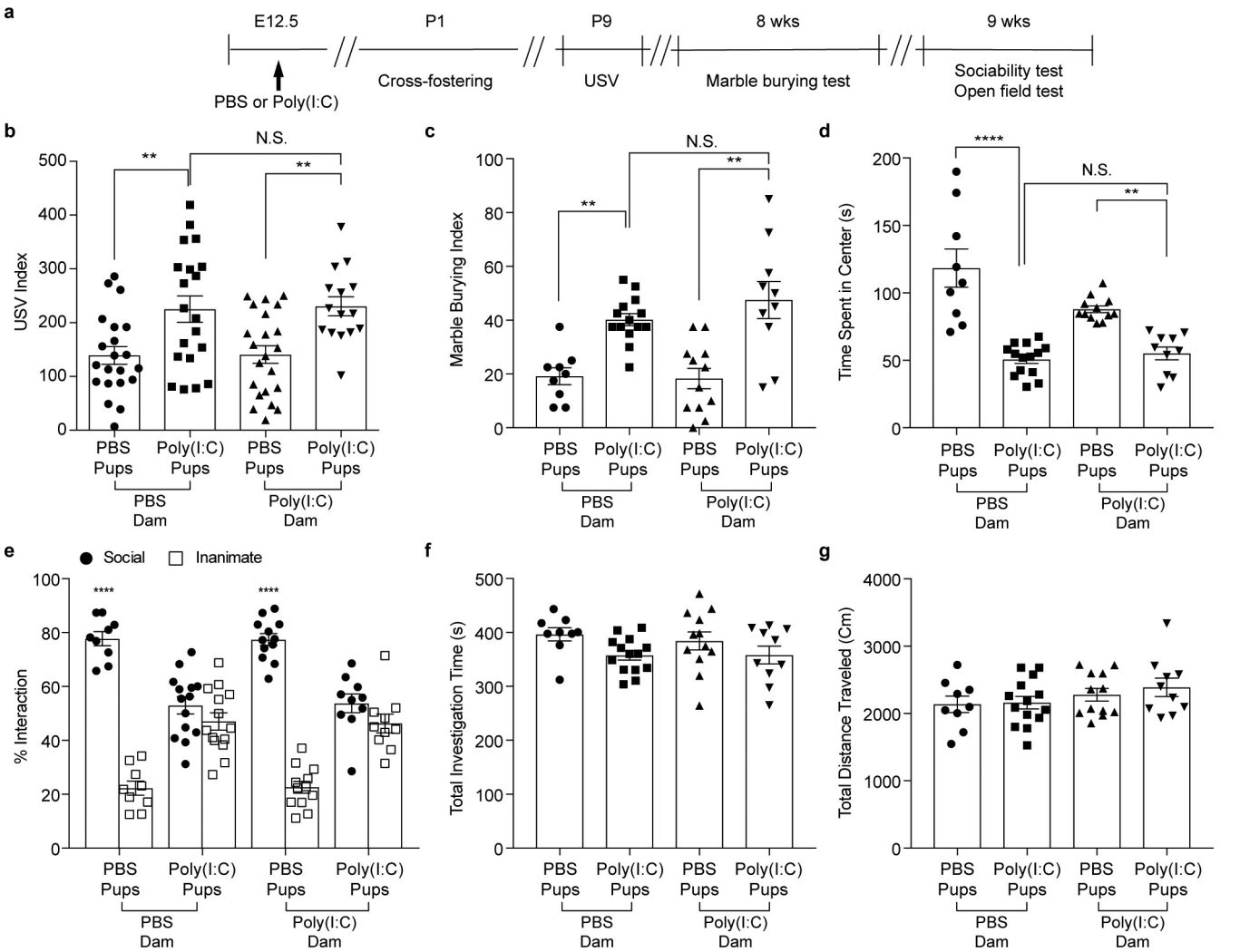


**Extended Data Figure 4 | Poly(I:C)-induced inflammation during pregnancy, not after giving birth, is critical in inducing MIA-associated behavioural abnormalities in offspring. a**, Schematic of the experimental design for cross-fostering experiments. **b**, USV index ($n = 21$, 20 (PBS dams; PBS, poly(I:C) pups); $n = 22$, 15 (poly(I:C) dams; PBS, poly(I:C) pups); 2–4 independent experiments). **c**–**g**, Marble burying index (**c**), time spent in the centre of an open field (**d**), and percentage of interaction (**e**), total investigation time (**f**), and total distance travelled (**g**) during the sociability test ($n = 9$, 14 (PBS dams; PBS, poly(I:C) pups); $n = 12$, 10 (poly(I:C) dams; PBS, poly(I:C) pups); 2 independent experiments). $^{**}P < 0.01$, $^{****}P < 0.0001$ calculated by one-way (**b**–**d**, **f**, **g**) and two-way (**e**) ANOVA with Tukey post hoc tests. NS, not significant. Graphs indicate mean ± s.e.m.

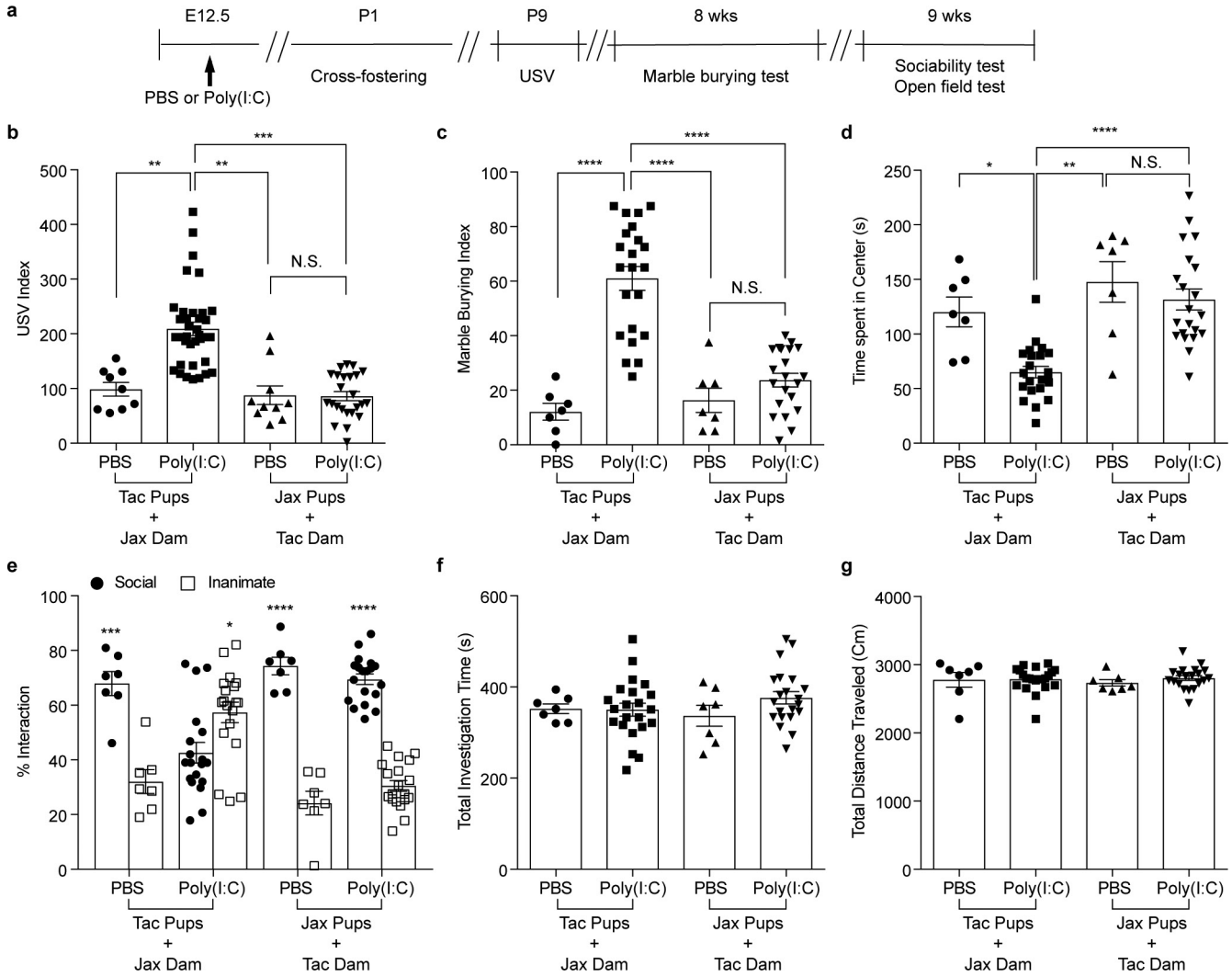


**Extended Data Figure 5 | Composition of maternal gut microbiota during pregnancy, not after giving birth, is critical in inducing MIA-associated behavioural abnormalities in offspring. a**, Schematic of the experimental design for cross-fostering experiments. **b**, USV index ($n = 9$, 36 (Tac pups with Jax dams; PBS, poly(I:C)); $n = 10$, 24 (Jax pups with Tac dams; PBS, poly(I:C)); 2–4 independent experiments). **c**–**g**, Marble burying index (**c**), time spent in the centre of an open field (**d**), and percentage of interaction (**e**), total investigation time (**f**), and total distance travelled (**g**) during the sociability test ($n = 7$, 22 (Tac pups with Jax dams; PBS, poly(I:C)); $n = 7$, 21 (Jax pups with Tac dams; PBS, poly(I:C)); 2 independent experiments). $^{*}P < 0.05$, $^{**}P < 0.01$, $^{***}P < 0.001$, $^{****}P < 0.0001$ calculated by one-way (**b**–**d**, **f**, **g**) and two-way (**e**) ANOVA with Tukey post hoc tests. NS, not significant. Graphs indicate mean ± s.e.m.

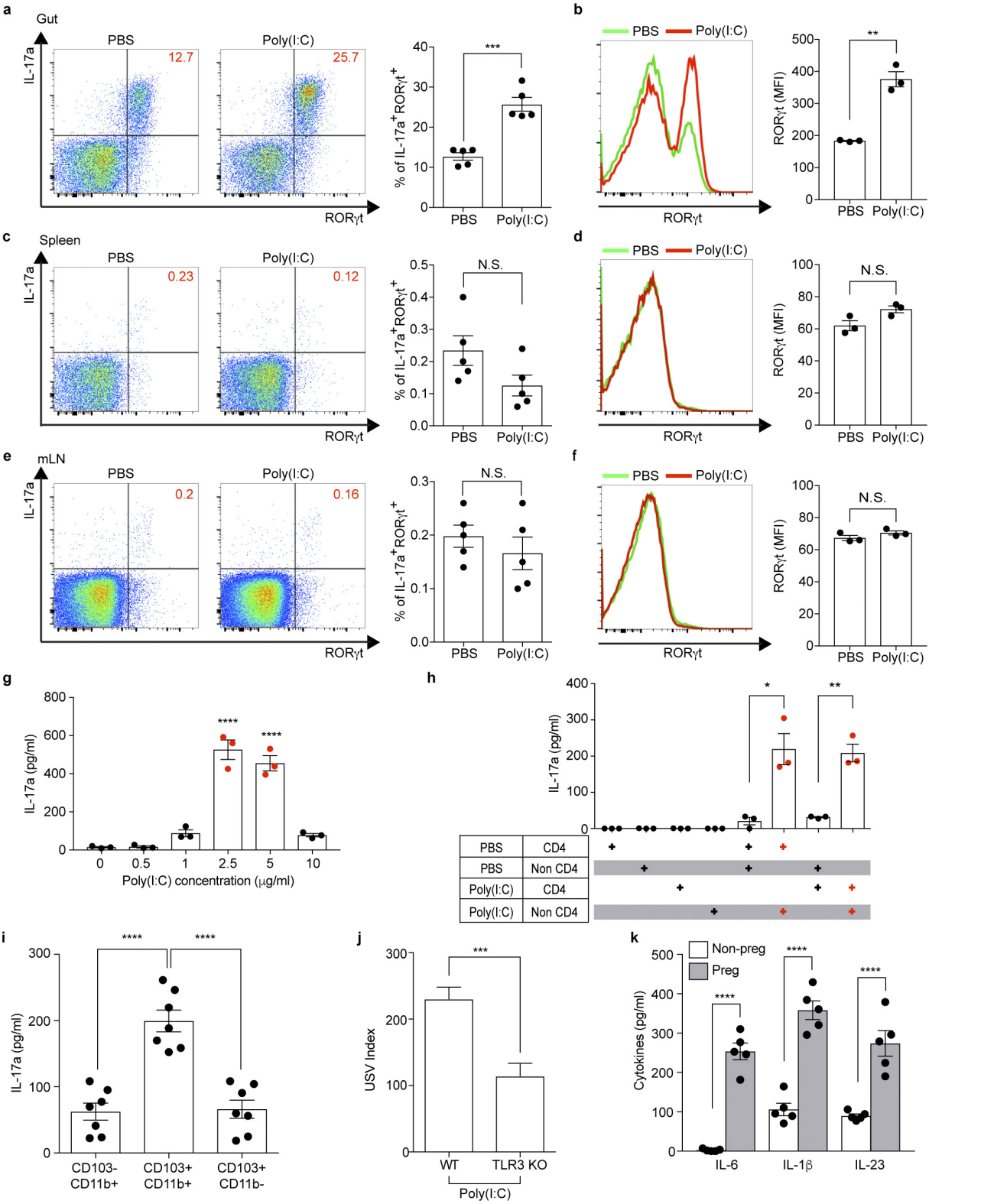


**Extended Data Figure 6 | CD11c$^+$ DCs stimulate gut T$_H$17 cells to produce high levels of IL-17a *ex vivo*.** **a**–**f**, Flow cytometry of CD4$^+$ T cells (gated on TCRβ$^+$CD4$^+$) stained intracellularly for IL-17a and RORγt. Mononuclear cells were collected at E14.5 from the gut ilea, spleens, and mesenteric lymph nodes (mLN) of PBS-, poly(I:C)-treated mice ($n = 5$ per group (**a**, **c**, **e**); $n = 3$ per group (**b**, **d**, **f**)). MFI denotes mean fluorescence intensity. **g**–**i**, Supernatant concentrations of IL-17a from mononuclear cells of the ilea in poly(I:C)-treated Tac dams (**g**) ($n = 3$ per group), from co-cultures of CD4$^+$ and non-CD4$^+$ cells of the ilea in PBS-, poly(I:C)-treated Tac dams (**h**) ($n = 3$ per group), or from co-cultures of CD4$^+$ and CD103$^-$CD11b$^+$, CD103$^+$CD11b$^+$ and CD103$^+$CD11b$^-$ (gated on MHCII$^+$CD11c$^+$) cells of the ilea in poly(I:C)-treated dams (**i**) ($n = 7$ per group). All cultures were isolated at E14.5 and stimulated *ex vivo* with poly(I:C) for 18 h (**g**, **h**) or for 48 h (**i**). Data are pooled from 2 (**g**, **h**) or 3 (**i**) independent experiments. **j**, USV index ($n = 16$, 17 (poly(I:C); wild type or TLR3-KO); 2 independent experiments). **k**, Supernatant concentrations of IL-6, IL-1β and IL-23 from cultures of CD11c$^+$ isolated at E14.5 from the ilea of poly(I:C)-treated non-pregnant or pregnant mice ($n = 5$ per group; 3 independent experiments). $^*P < 0.05$, $^{**}P < 0.01$, $^{***}P < 0.001$ and $^{****}P < 0.0001$ calculated by Student's *t*-test (**a**–**f**, **j**, **k**) and one-way ANOVA (**g**–**i**) with Tukey post hoc tests. NS, not significant. Graphs indicate mean ± s.e.m.

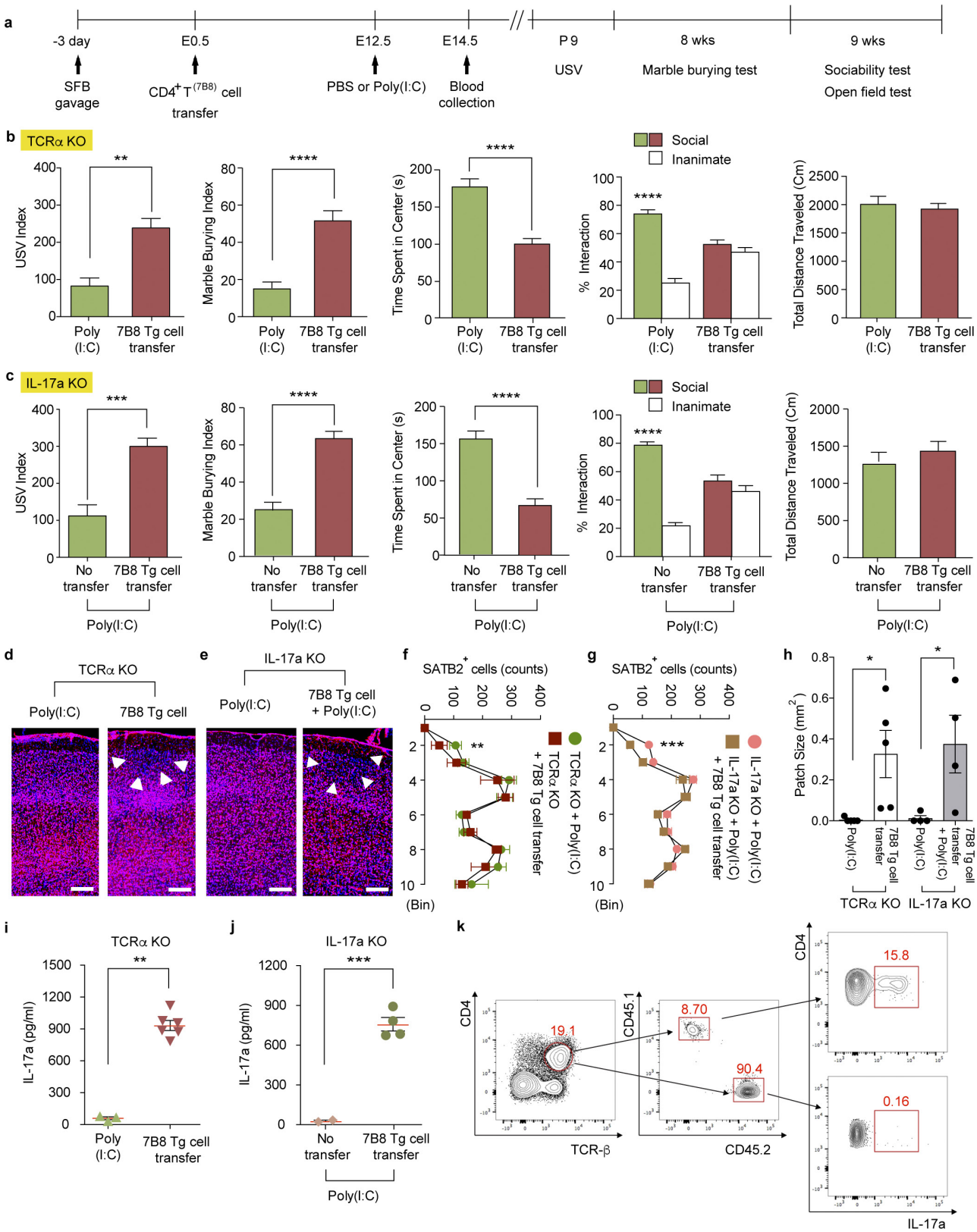


**Extended Data Figure 7** | See next page for caption.

**Extended Data Figure 7 | SFB-specific 7B8-Tg CD4$^+$ T cells produce IL-17a upon transfer to MIA-exposed pregnant mothers. a**, Schematic of the experimental design. **b**, **c**, Both TCRα-KO and IL-17a-KO females, with or without adoptive transfers of 7B8-Tg-derived CD4$^+$ T cells, were crossed with wild-type C57BL/6 males to produce heterozygous wild-type offspring. USV index ($n = 16$, 30 (TCRα-KO; poly(I:C), 7B8-Tg T cell transfer); $n = 23$, 23 (IL-17a-KO; poly(I:C), 7B8-Tg T cell transfer + poly(I:C)), marble burying index, time spent in the centre of an open field, and percentage interaction and total distance travelled during the sociability test of TCRα-KO (**b**) or IL-17a-KO (**c**) offspring ($n = 12$, 15 (TCRα-KO; poly(I:C), 7B8-Tg T cell transfer); $n = 12$, 14 (IL-17a-KO; poly(I:C), 7B8-Tg T cell transfer + poly(I:C)). Data pooled from 2–3 independent experiments. **d**, **e**, Representative SATB2 staining in the cortex of the animals prepared as in **a**. Arrowheads indicate cortical patches. Scale bars, 100 μm. **f**, **g**, Quantification of SATB2$^+$ cells ($n = 7$, 6 (TCRα-KO; poly(I:C), 7B8-Tg T cell transfer); $n = 6$, 7 (IL-17a-KO; poly(I:C), 7B8-Tg T cell transfer + poly(I:C)). **h**, Cortical patch size ($n = 5$, 5 (TCRα-KO; poly(I:C), 7B8-Tg T cell transfer); $n = 4$, 4 (IL-17a-KO; poly(I:C), 7B8-Tg T cell transfer + poly(I:C)). **i**, **j**, IL-17a concentrations in maternal plasma collected at E14.5. **k**, Flow cytometry of ileal CD4$^+$ T cells (gated on CD4$^+$TCRβ$^+$) stained intracellularly for IL-17a. Mononuclear cells were collected from small intestines of poly(I:C)-treated IL-17a-KO mothers transferred with 7B8-Tg CD4$^+$ T cells. CD45.1$^+$ cells refer to donor cells and CD45.2$^+$ to recipient cells. $^*P < 0.05$, $^{**}P < 0.01$, $^{***}P < 0.001$, $^{****}P < 0.0001$ calculated by Student's *t*-test (**b**, **c**, **h**–**j**) and one-way (**f**, **g**) ANOVA with Sidak post hoc tests. Graphs indicate mean ± s.e.m.

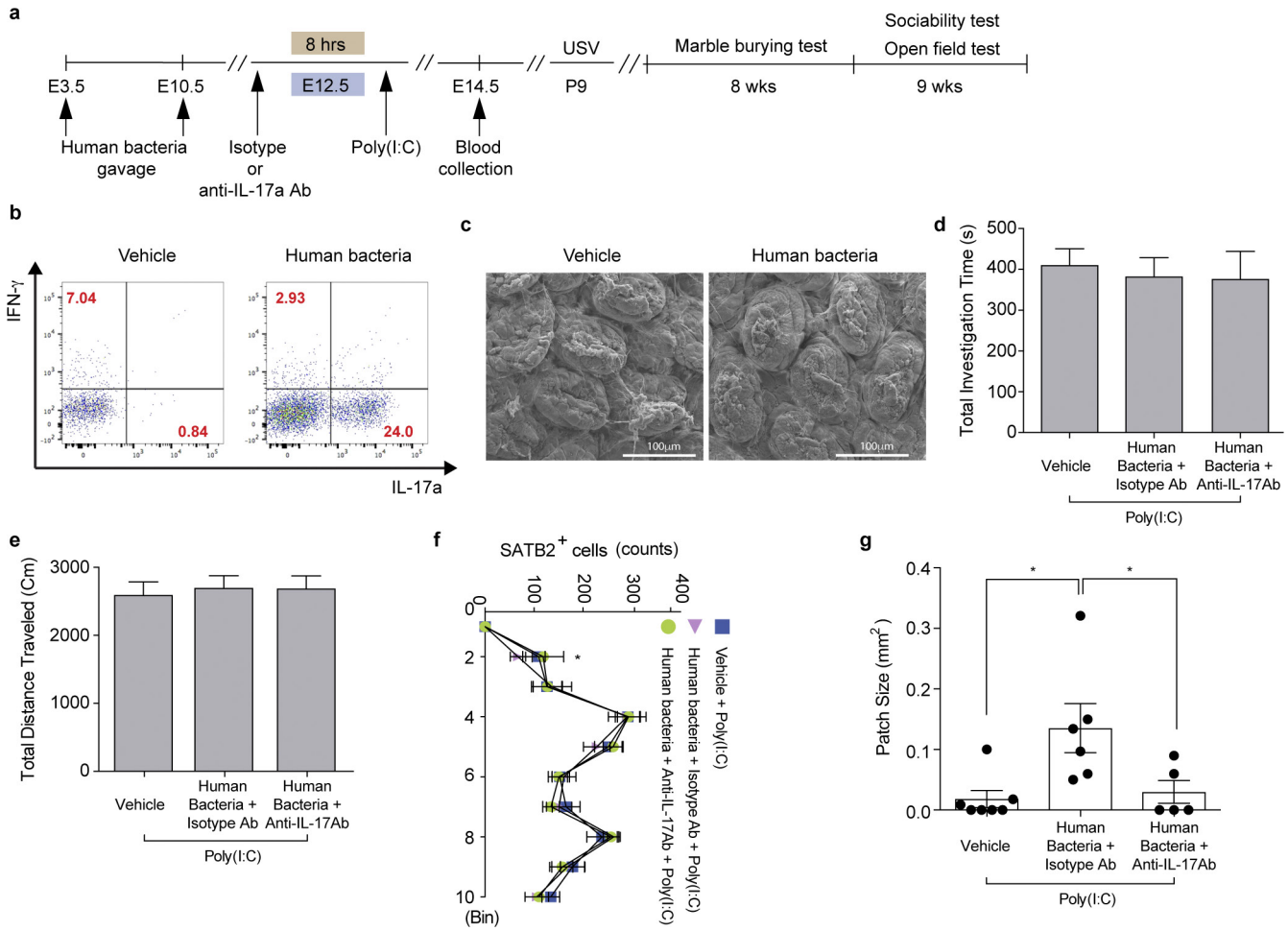


**Extended Data Figure 8 | A mix of twenty human commensals induces colonic $T_H17$ cell differentiation in SFB-absent Jax mice. a**, Schematic of the experimental design. **b**, Flow cytometry of $CD4^+$ T cells (gated on $CD4^+TCR\beta^+$) stained intracellularly for IL-17a and RORγt. Mononuclear cells were collected from colons of poly(I:C)-treated Jax mothers with/without human bacteria gavage. **c**, Representative scanning electron microscopy images of epithelial surfaces in the ilea from 2 independent experiments. **d**, **e**, Total interaction time (**d**), and total distance travelled (**e**) during the sociability test of adult offspring described in **a** ($n = 23$, vehicle-gavaged only; 22, human-bacteria-gavaged + isotype control antibody; 13, human-bacteria-gavaged + anti-IL-17a antibody; 4 independent experiments). **f**–**g**, Quantification of $SATB2^+$ cells ($n = 5$ per group) and cortical patch size ($n = 7, 6, 5$ (poly(I:C); vehicle-treated Jax, human-bacteria-gavaged Jax with isotype control antibody, human-bacteria-gavaged Jax with anti-IL-17a antibody). $^*P < 0.05$ calculated by one-way (**d**, **e**, **g**) and two-way (**f**) ANOVA with Tukey post hoc test. Graphs indicate mean ± s.e.m.

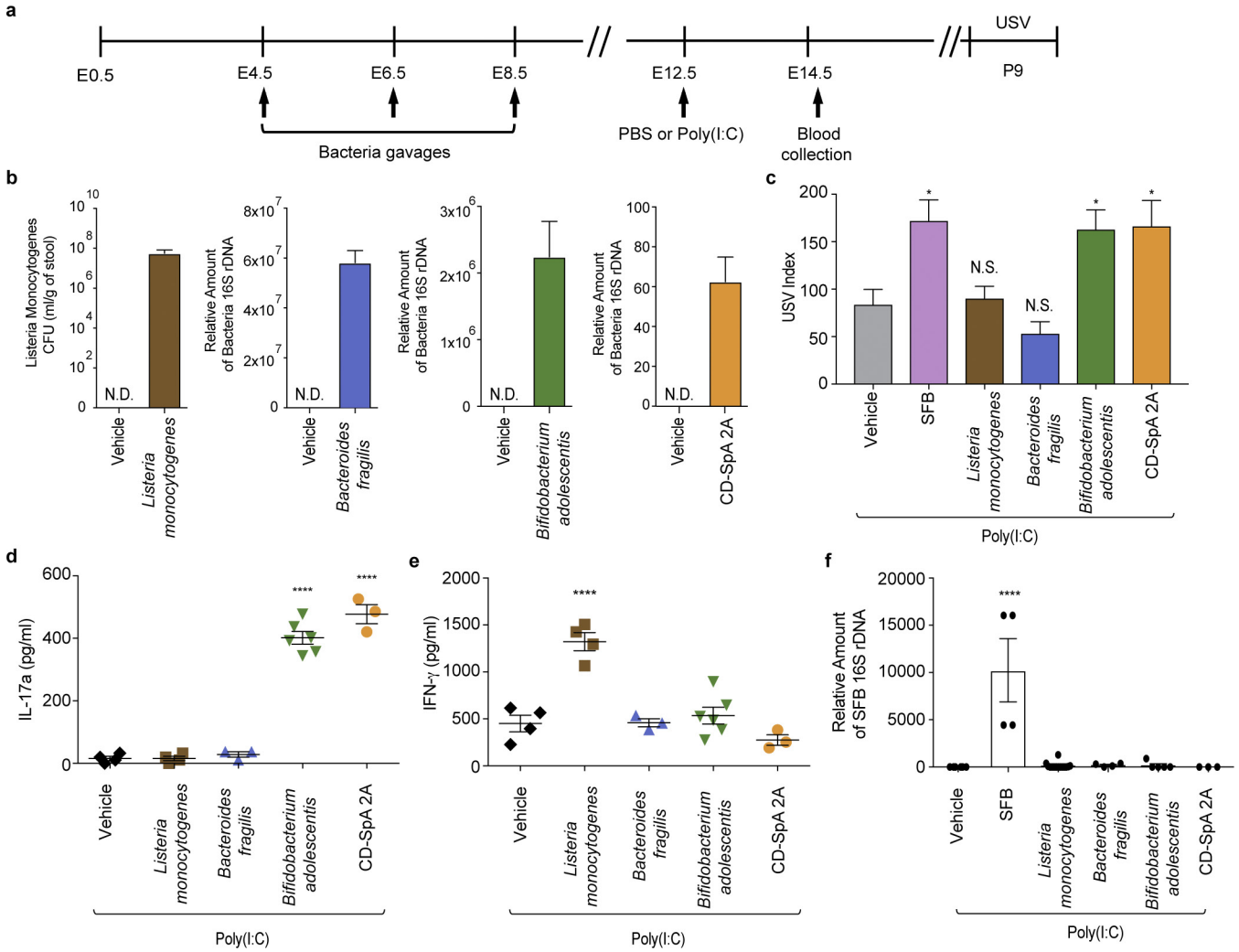


**Extended Data Figure 9 | The IL-17a pathway promotes abnormal behavioural phenotypes in MIA offspring born to mice colonized with human commensal bacteria. a**, Schematic representation of the experimental design. **b**, Quantification of bacterial colonization levels through colony forming unit (CFU) counts or qPCR analyses. **c**, USV index ($n = 13, 12, 28, 16, 17, 14$ (poly(I:C); vehicle, SFB, *Listeria monocytogenes*, *Bacteroides fragilis*, *Bifidobacterium adolescentis*, CD-SpA 2A). **d**, **e**, Maternal plasma concentrations of IL-17a and IFNγ at E14.5 ($n = 4, 4, 3, 6, 3$ (poly(I:C); vehicle, *Listeria monocytogenes*, *Bacteroides fragilis*, *Bifidobacterium adolescentis*, CD-SpA 2A). **f**, qPCR analysis measuring relative SFB levels in Jax mice gavaged with various bacteria; from two independent experiments. $^{*}P < 0.05$, $^{****}P < 0.0001$ calculated by one-way (**c**–**f**) ANOVA with Tukey post hoc tests and Student's *t*-test (**b**). ND, not determined. NS, not significant. Graphs indicate mean ± s.e.m.

nature research

Corresponding Author: Jun R. Huh

Date: June 7, 2017

# Life Sciences Reporting Summary

Nature Research wishes to improve the reproducibility of the work we publish. This form is published with all life science papers and is intended to promote consistency and transparency in reporting. All life sciences submissions use this form; while some list items might not apply to an individual manuscript, all fields must be completed for clarity.

For further information on the points included in this form, see Reporting Life Sciences Research. For further information on Nature Research policies, including our data availability policy, see Authors & Referees and the Editorial Policy Checklist.

## Experimental design

1. Sample size

   Describe how sample size was determined.

   Sample sizes were determined based on a similarly conducted previous study. (Material & Methods p53, Ref.8)

2. Data exclusions

   Describe any data exclusions.

   We have not excluded any data.

3. Replication

   Describe whether the experimental findings were reliably reproduced.

   Experimental findings were reliably reproduced.

4. Randomization

   Describe how samples/organisms/participants were allocated into experimental groups.

   Subject animals were randomly assigned to experimental groups.

5. Blinding

   Describe whether the investigators were blinded to group allocation during data collection and/or analysis.

   Blinding was done for all the behavioral experiments except for the experiments with human bacteria (Material & Methods, p45).

Note: all studies involving animals and/or human research participants must disclose whether blinding and randomization were used.

6. Statistical parameters

   For all figures and tables that use statistical methods, confirm that the following items are present in relevant figure legends (or the Methods section if additional space is needed).

| n/a | Confirmed | |
|---|---|---|
| ☐ | ☒ | The exact sample size (*n*) for each experimental group/condition, given as a discrete number and unit of measurement (animals, litters, cultures, etc.) |
| ☐ | ☒ | A description of how samples were collected, noting whether measurements were taken from distinct samples or whether the same sample was measured repeatedly. |
| ☐ | ☒ | A statement indicating how many times each experiment was replicated |
| ☐ | ☒ | The statistical test(s) used and whether they are one- or two-sided (note: only common tests should be described solely by name; more complex techniques should be described in the Methods section) |
| ☐ | ☒ | A description of any assumptions or corrections, such as an adjustment for multiple comparisons |
| ☐ | ☒ | The test results (e.g. *p* values) given as exact values whenever possible and with confidence intervals noted |
| ☐ | ☒ | A summary of the descriptive statistics, including central tendency (e.g. median, mean) and variation (e.g. standard deviation, interquartile range) |
| ☐ | ☒ | Clearly defined error bars |

*See the web collection on statistics for biologists for further resources and guidance.*

## Software

Policy information about availability of computer code

7. Software

   Describe the software used to analyze the data in this study.

   GraphPad Prism 6

For all studies, we encourage code deposition in a community repository (e.g. GitHub). Authors must make computer code available to editors and reviewers upon request. The *Nature Methods* guidance for providing algorithms and software for publication may be useful for any submission.

## Materials and reagents

Policy information about availability of materials

8. Materials availability

| | |
|---|---|
| Indicate whether there are restrictions on availability of unique materials or if these materials are only available for distribution by a for-profit company. | No unique material was used. |

9. Antibodies

| | |
|---|---|
| Describe the antibodies used and how they were validated for use in the system under study (i.e. assay and species). | Pacific Blueconjugated anti-CD4 (RM-5), PerCP-Cy5.5-conjugated anti-CD8a (53-6.7), APC-Cy7-conjugated anti-TCRβ (H57-597), FITC-conjugated anti-CD62L (MEL-14), APCconjugated anti-CD44 (IM7), PE-conjugated-CD25 (PC61.5), PerCP-Cy5.5-conjugated-CD19 (eBio1D3), APC-conjugated anti-CD45.1 (A20), FITC-conjugated anti-CD45.2(104), Pacific Blue conjugated anti-CD11c (N418), FITC conjugated-anti-CD11b (M1/70), PerCP-Cy5.5-conjugated-anti-CD103 (2E7) (eBioscience), Biotin-conjugated Vβ14 (14-2) (BD phamigen) and PE-Cy7-conjugated-Streptavidin (Thermo Fisher Scientific). Cells were further stained intracellularly with APC-conjugated anti-RORγ (B2D) (eBioscience) and PE-Cy7-conjugated anti-IL-17a (eBio17B7) (eBioscience) ; (Material & methods, p41) |

10. Eukaryotic cell lines

| | |
|---|---|
| a. State the source of each eukaryotic cell line used. | No eukaryotic cell lines was used. |
| b. Describe the method of cell line authentication used. | *Describe the authentication procedures for each cell line used OR declare that none of the cell lines used have been authenticated OR state that no eukaryotic cell lines were used.* |
| c. Report whether the cell lines were tested for mycoplasma contamination. | *Confirm that all cell lines tested negative for mycoplasma contamination OR describe the results of the testing for mycoplasma contamination OR declare that the cell lines were not tested for mycoplasma contamination OR state that no eukaryotic cell lines were used.* |
| d. If any of the cell lines used in the paper are listed in the database of commonly misidentified cell lines maintained by ICLAC, provide a scientific rationale for their use. | *Provide a rationale for the use of commonly misidentified cell lines OR state that no commonly misidentified cell lines were used.* |

## Animals and human research participants

Policy information about studies involving animals; when reporting animal research, follow the ARRIVE guidelines

11. Description of research animals

| | |
|---|---|
| Provide details on animals and/or animal-derived materials used in the study. | All experiments were performed according to Guide for the Care and Use of Laboratory Animals and were approved by the National Institutes of Health and the Committee and Animal Care at University of Massachusetts Medical School. C57BL/6, tcra KO, tlr3 KO, il17a gfp and SFB-specific TCR Tg (7B8) mice were purchased from Taconic biosciences and Jackson Laboratory. To induce MIA phenotypes, SFB were introduced into mice purchased from Jackson laboratory. Il17aKO mice were described elsewhere (ref. 25) |

Policy information about studies involving human research participants

12. Description of human research participants

| | |
|---|---|
| Describe the covariate-relevant population characteristics of the human research participants. | The study did not involve human research participants. |

Corresponding Author: Jun R. Huh

Date: June 22, 2017

# Flow Cytometry Reporting Summary

Form fields will expand as needed. Please do not leave fields blank.

## Data presentation

For all flow cytometry data, confirm that:

☒ 1. The axis labels state the marker and fluorochrome used (e.g. CD4-FITC).

☒ 2. The axis scales are clearly visible. Include numbers along axes only for bottom left plot of group (a 'group' is an analysis of identical markers).

☒ 3. All plots are contour plots with outliers or pseudocolor plots.

☒ 4. A numerical value for number of cells or percentage (with statistics) is provided.

## Methodological details

| | |
|---|---|
| 5. Describe the sample preparation. | For mononuclear cell isolations, both mesenteric fat tissues and Peyer's patches were carefully removed from intestinal tissues. Terminal ileal or colonic tissues were incubated in 5 mM EDTA in PBS containing 1 mM DTT at 37°C on a shaker (200 rpm) for 20 min. Tissues were washed one more time. Tissues were then further digested for 30 min at 37oC in RPMI containing 10% fetal bovine serum, 1.0 mg/ml Collagenase D (Roche) and 100 µg/ml DNase I (Sigma). Digested tissues were then filtered using a 100 µm cell strainer and incubated for additional 10 min at 37oC. Mononuclear cells were isolated from an interphase of percoll gradients (40:80 gradient). |
| 6. Identify the instrument used for data collection. | LSRII (BD Biosciences), Aria II (BD Biosciences) |
| 7. Describe the software used to collect and analyze the flow cytometry data. | We used FACS DIVA (BD)to collect samples and Flowjo (Tree Star) for analysis. |
| 8. Describe the abundance of the relevant cell populations within post-sort fractions. | After cell sorting, we checked to purity and cell numbers by FACS Aria (BD Bioscience). |
| 9. Describe the gating strategy used. | Singlet cells were gated on FSC-A/FSC-W and Live/Dead on DAPI. All T cells were gated on FSC/SSC, CD4+/CD8-/CD19-, CD4+/TCR-b +, RORgt+/IL-17a+.<br>7B8 Tg cells for adoptive transfer were identified as: singlet cells were gated on FSC-A/FSC-W and Live/Dead on DAPI. All cells were gated on FSC/SSC and then CD4+/CD8-/CD19-, Vb14+/CD25-, CD62L+/CD44-.<br>For sorting intestinal DCs: singlet cells gated on FSC-A/FSC-W and Live/Dead on DAPI. All cells were gated on FSC/SSC, CD11c+/MHCII +, and sorted based on the surface expression of CD11b and CD103.<br>For sorting intestinal GFP+ or GFP- T cells: singlet cells were gated on FSC-A/FSC-W and Live/Dead on DAPI. All cells were further gated on FSC/SSC, CD4+/CD19-, followed by GFP expression. |

Tick this box to confirm that a figure exemplifying the gating strategy is provided in the Supplementary Information. ☐